

Section 2 Plasma Physics

Chapter 1 Plasma Dynamics

Chapter 1. Plasma Dynamics

Academic and Research Staff

Professor Abraham Bers, Professor Bruno Coppi, Dr. Stefano Migliuolo, Dr. Abhay K. Ram, Dr. Linda E. Sugiyama, Ivan Mastovsky

Visiting Scientists and Research Affiliates

Dr. Augusta Airoidi, Dr. Didier Benisti,¹ Dr. Giuseppe Bertin, Dr. Francesca Bombarda, Dr. Madurja P. Bora, Franco Carpignano, Dr. Vladimir Fuchs,² Dr. Giovanna Cennachi, Dmitri Laveder, Dr. Riccardo Maggiora, Dr. Francesco Pegoraro, Marco Ricitelli, George M. Svolos, Dr. Motohiko Tanaka, Dr. Joachim S. Theilhaber³

Graduate Students

Palmyra E. Catravas, William S. Daughton, Darin R. Ernst, Ronald J. Focia, Felicissimo W. Galicia, Gregory E. Penn, Caterina Riconda, Steven D. Schultz, Luigi Vacca, Kenneth C. Wu

Undergraduate Students

Gianmarco Felice, Ming-Hui Kuang, Peter Ouyang, Evan Reich

Support Staff

Laura M. Von Bosau

1.1 Non-perturbative Beam Characterization with a Microwiggler

Sponsor

U.S. Navy - Office of Naval Research
Grant N00014-90-J-4130

Project Staff

Professor Hermann A. Haus, Professor Jonathan S. Wurtele,⁴ Ivan Mastovsky, Palmyra E. Catravas

The late George Bekefi was the principal investigator for this project from 1989-1995. In the past year, we have performed first measurements of a single-shot technique for characterizing the properties of a 50 MeV electron beam with a

microwiggler.⁵ Experimental work in this area is typically limited by poor resolution and the difficulty of distinguishing between numerous inherent spontaneous emission broadening mechanisms such as energy spread, beam divergence, off-axis electron propagation, beam trajectory errors and collection angle effects. The MIT Microwiggler is a planar, pulsed electromagnet with individually tunable half-periods which generates a peak on-axis field of 0.45 Tesla. Through its compact size, extensive profile tunability, adjustable field strength, long length and short period (8.8 mm), the microwiggler offers unique opportunities for such an application, particularly in sensitivity of emissions to beam parameters, and in the wavelength of emission (532 nm at approximately 50 MeV), where a wide variety of optical diagnostics are available. The response of the spontaneous emission-based technique to

¹ Programme Lavoisier Fellow, France.

² Centre Canadien de Fusion Magnétique (CCFM), Québec, Canada.

³ IBM Corporation, Waltham, Massachusetts.

⁴ Presently at the Lawrence Berkeley Laboratory, Berkeley, California.

⁵ X.Z. Qiu, P. Catravas, X.-J. Wang, M. Babzien, I. Ben-Zvi, J. Fang, W. Graves, Y. Liu, R. Mallone, I. Mastovsky, Z. Segalov, J. Sheehan, R. Stoner, and J.S. Wurtele, "Experiments in Non-perturbative Electron Beam Characterization with the MIT Microwiggler at the Accelerator Test Facility at BNL." Eighteenth International Free Electron Laser Conference, Rome, Italy, 1996, forthcoming.

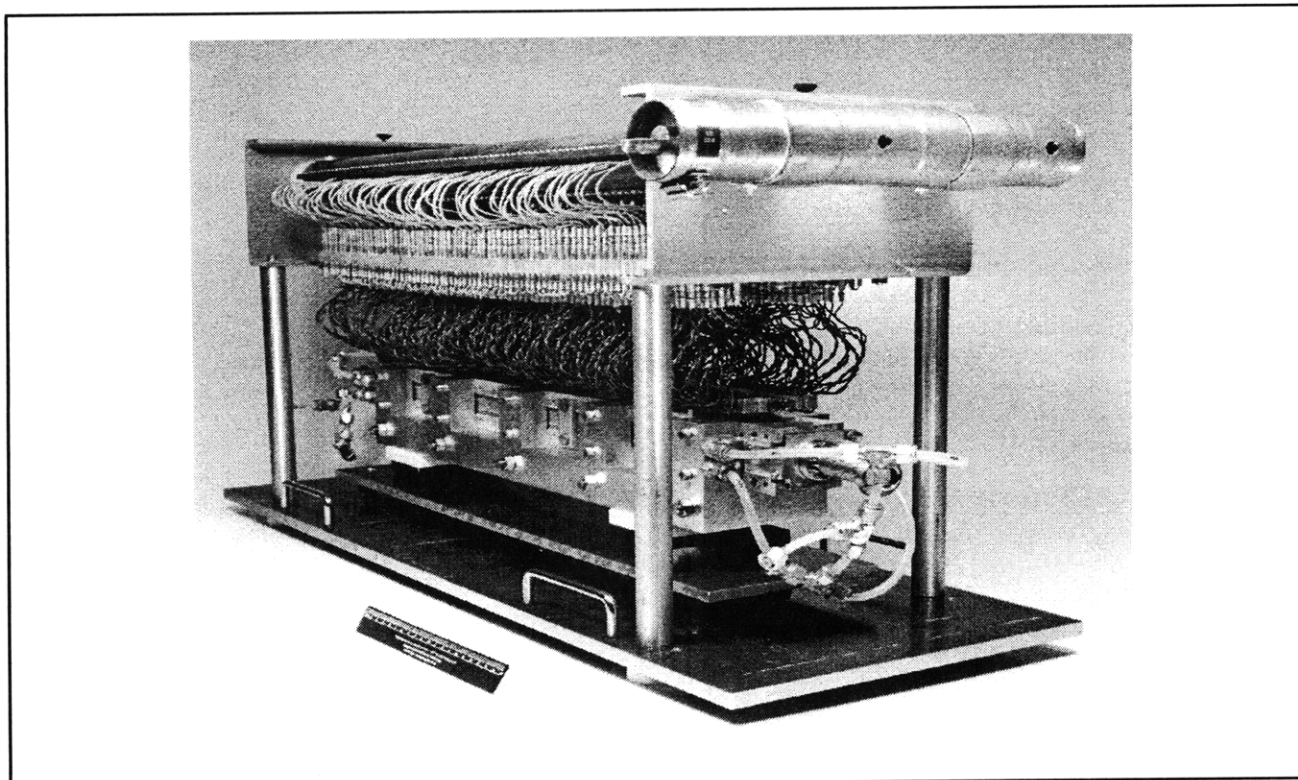


Figure 1. The MIT Microwiggler.

beam parameters was demonstrated with a systematic series of experiments at the Accelerator Test Facility at the Brookhaven National Laboratory. An estimate of beam divergence was obtained from the measurements.

1.1.1 The Microwiggler

High field precision in short-period wigglers is difficult to achieve. Mechanical tolerances and other coil-to-coil variations become sufficiently large on the scale of the wiggler period that they translate easily into field errors of harmful amplitude. The severity of the problem compounds with wiggler length, and curtails efficiency through deleterious increases in electron beam walk-off and energy spread. We have employed a novel approach to reducing wiggler field errors in which extensive tunability is controlled through a rigorous tuning procedure.

Wiggler design, construction (figure 1) and tuning algorithm are detailed in our previous work.⁶ In order to completely characterize the microwiggler field characteristics, a comprehensive battery of field measurements was performed, including peak amplitudes, peak positions, magnetic center positions, full wiggler profile and spatial harmonic content, and coil temporal response. The best result using the novel tuning regimen for rms spread in peak amplitudes was 0.08 percent, the lowest ever achieved in a sub-cm period magnetic field.⁷

1.1.2 Experiments in Non-perturbative Electron Beam Characterization

The setup for spontaneous emission studies of the electron beam is simple and efficient. The spatial profile of spontaneous emission into a Cerenkov Cone is recorded using a narrow bandwidth interference filter and a CCD camera. The radius of the cone depends on the interference filter central

⁶ R. Stoner and G. Bekefi, "A 70-Period High-Precision Microwiggler for Free Electron Lasers," *IEEE J. Quant. Electron.* 31: 1158-1165 (1995).

⁷ P. Catravas, R. Stoner, G. Bekefi, J. Blastos, D. Sisson, I. Mastovsky, G. Bekefi, A. Fisher, and X.-J. Wang, "MIT Microwiggler for Free Electron Laser Applications," *Proceedings of the 1995 Particle Accelerator Conference*.

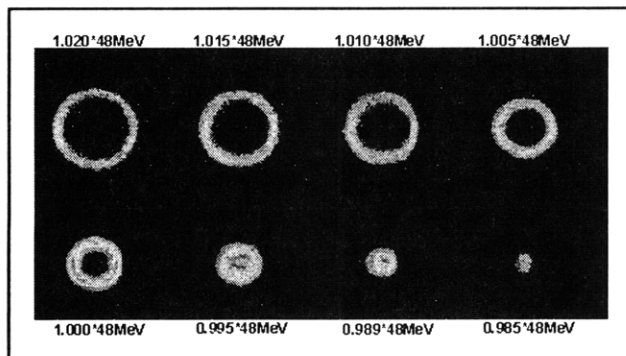


Figure 2. CCD images showing dependence on beam energy of S.E. cones with a 1 nm bandwidth. The wiggler plane corresponds to the vertical axis.

wavelength and electron beam energy, while the cone width is determined by energy spread and divergence broadening and the number of periods in the wiggler. Systematic measurements of the cone width over a range in beam energy, energy spread, tuning parameters and wiggler field strength have been performed (figure 2). Simple analytic expressions for the contribution of natural linewidth, energy spread and divergence were derived, and it was found that by looking at large angles, a figure for beam divergence could be extracted directly from a single shot measurement.

Using our microwiggler, we are collaborating with the Accelerator Test Facility at Brookhaven National Laboratory to perform FEL research, including experiments in self-amplified spontaneous emission (SASE). The technique developed in non-perturbative beam characterization is useful for estimating beam emittance, as an aid in matching the beam into the wiggler and provides direct, immediate feedback during beam tuning and optimization. It can be applied to the immediate research, as well as extended to more general applications.

1.1.3 Publications

Babzien, M., I. Ben-Zvi, P. Catravas, J. Fang, W. Graves, Z. Segalov, and X.-J. Wang. "Optical Diagnostics for the ATF Microundulator FEL." *Nucl. Instr. Meth.* A375: 421 (1996).

Catravas, P., R. Stoner, and G. Bekefi. "Characteristics of the MIT Microwiggler for Free Electron Laser Applications." *Nucl. Instr. Meth.* A375: 412 (1996).

Qiu, X.Z., P. Catravas, X.-J. Wang, M. Babzien, I. Ben-Zvi, J. Fang, W. Graves, Y. Liu, R. Mallone, I. Mastovsky, Z. Segalov, J. Sheehan, R. Stoner, and J.S. Wurtele. "Experiments in Non-perturbative Electron Beam Characterization

with the MIT Microwiggler at the Accelerator Test Facility at BNL." Eighteenth International Free Electron Laser Conference, Rome, Italy, 1996. Forthcoming.

1.2 Plasma Wave Interactions - RF Heating and Current Generation

1.2.1 Introduction

The research of this group is concerned with both basic and applied problems in the electrodynamics of plasmas. Basic to the electrodynamics of plasmas are interactions of various plasma waves with the constituent charged particles of the plasma, as well as interactions between different plasma waves. These interactions are generally nonlinear and entail studies of the evolution of coherent structures (e.g., solitons) as well as chaotic dynamics (low-dimensional and spatiotemporal chaos). Applied studies of current interest address problems in magnetic confinement fusion, space plasma physics, and inertial confinement fusion. In particular: RF heating and current drive in magnetically confined plasmas; understanding the energization of O^+ and H^+ ions from the ionosphere to the magnetosphere; and light scattering instabilities in laser-plasma interactions.

Section 1.2.2 describes our discovery of a new mechanism for coherent and chaotic acceleration of ions. This can be applied to explaining the observed energetic ions in the ionosphere, which is what stimulated the study, but can also be of importance as a new means of plasma heating. In the former case, the plasma fields acting on the ions originate from plasma instabilities in the upper ionosphere, while in the latter case the required plasma fields could be driven from sources external to the plasma. Section 1.2.3 relates to our work on tokamak improvements by the synergistic use of the intrinsic current due to the bootstrap effect and the use of external RF power. This study involves simulations that couple velocity and configuration space dynamics. Sections 1.2.4 and 1.2.5 describe our continuing study of mode conversion in the ion-cyclotron regime, specifically from a fast Alfvén wave (FAW) to an ion-Bernstein wave (IBW). The results generalize our previous work in including the effects of poloidal variation in the fields as well as the effect of shear in the confining magnetic field (1.2.4) and establishing the conditions under which mode-converted IBWs can be used to generate currents in the plasma (1.2.5). Section 1.2.6 gives the first results on our new proposal for heating and current drive in the National Spherical Tokamak Experiment (NSTX)—a new national facility for

"spherical" tokamak research. Our proposal consists of the use of mode conversion in the electron-cyclotron range of frequencies, from an externally-coupled-to-extraordinary wave to an electron-Bernstein wave.

1.2.2 Ion Dynamics in Multiple Electrostatic Waves in a Magnetic Field

Sponsors

National Science Foundation
Contract ATM 94-24282
U.S. Department of Energy
Contract DE-FG02-91-ER-54109

Project Staff

Professor Abraham Bers, Dr. Abhay K. Ram, Dr. Didier Benisti, Dr. Joachim S. Theilhaber, Felicisimo W. Galicia

A very general theoretical study of the dynamics of ions acted upon by electrostatic waves propagating across a uniform magnetic field has been performed. This has applications in tokamak heating⁸ and in providing a mechanism whereby ionospheric ions can be accelerated.⁹ The main result is the discovery of a new mechanism of coherent acceleration which occurs with at least two waves in a magnetic field. The coherent acceleration mechanism allows the energization of very low energy particles, which cannot be accelerated by only one wave. It also allows particles to access much higher energies than with only one wave.

The motion of an ion of mass m and charge q in a uniform magnetic field $\vec{B} = B_0 \hat{z}$ and being perturbed by a spectrum of electrostatic waves $\vec{E} = \hat{x} \sum_{i=1}^N E_i \sin(k_i x - \omega_i t + \varphi_i)$ is given by

$$\frac{d^2 x}{dt^2} + \Omega^2 x = \frac{q}{m} \sum_{i=1}^N E_i \sin(k_i x - \omega_i t + \varphi_i) \quad (1)$$

where $\Omega = qB_0/m$ is the ion cyclotron frequency. We normalize time to Ω^{-1} and length to k_1^{-1} and define the dimensionless variables $X = k_1 x$ and $\tau = \Omega t$. We then switch to the normalized action-angle variables of the linear oscillator. The action is $I = X^2/2 + \dot{X}^2/2$, where $\dot{X} = dX/d\tau$. The angle θ is defined by $X = \rho \sin \theta$, $\dot{X} = \rho \cos \theta$, where $\rho = \sqrt{2I}$ is the normalized Larmor radius. In action-angle variables, the Hamiltonian corresponding to (1) is

$$H = I + \sum_{i=1}^N \varepsilon_i \cos(k_i \rho \sin \theta - \nu_i \tau + \varphi_i) \quad (2)$$

where $\varepsilon_i = qE_i k_1 / (m\Omega^2)$ is the normalized electric field amplitude. There is a finite region in energy inside which the dynamics defined by the Hamiltonian equation (2) can be chaotic. The bounds in energy of the stochastic region have been defined,¹⁰ for the case of one "off-resonance" wave, i.e., a wave whose frequency is not an integer multiple of the ion cyclotron frequency. The lower bound in energy of the stochastic region corresponds to

$$\rho = \nu - \sqrt{\varepsilon} \quad (3)$$

This bound remains essentially unchanged in the case of more than one wave. The upper bound of the stochastic region corresponds to

$$\rho = (4\varepsilon\nu)^{2/3} (2/\pi)^{1/3}. \quad (4)$$

In the case of one off-resonance wave, equation (3) yields the minimum energy an ion needs to have in order to be accelerated by the wave, and equation (4) yields the maximum energy an ion can get through stochastic acceleration.

In the case of one "on-resonance" wave, i.e., a wave whose frequency is an integer multiple of the ion cyclotron frequency, the situation is qualitatively different, as the ion phase space is filled with a web structure, for any non-zero value of the wave ampli-

⁸ H. Pacher, C. Gormezano, W. Hess, G. Ichtchenko, R. Magne, T.-K. Nguyen, G.W. Pacher, F. Söldner, G. Tonon, and J.-G. Wegrowe, "Heating in Toroidal Plasmas II," *Proceedings of the 2nd Joint Grenoble-Varenna International Symposium*, Como, Italy, September 3-12, 1980, eds. E. Canobbio, H.P. Eubank, G.G. Leotta, A. Malein, and E. Sindoni, p. 329.

⁹ J.L. Vago, P.M. Kintner, S. Chesney, R.L. Arnoldy, K.A. Lynch, T.E. Moore, and C.J. Pollock, *J. Geophys. Res.* 97: 16935 (1992).

¹⁰ C.F.F. Karney and A. Bers, *Phys. Rev. Lett.* 39: 550 (1977); C.F.F. Karney, *Phys. Fluids* 21: 1584 (1978); C.F.F. Karney, *Phys. Fluids* 22: 2188 (1979).

tude.¹¹ In principle, a particle could gain an infinite energy through the web structure. Nevertheless, the web structure also has a lower bound in energy.¹² Moreover, this lower bound increases with increasing wave amplitude (see figure 3). This implies that the existence of a web structure does not dramatically change the bound equation (3), especially for a wave at a high harmonic of the cyclotron frequency. Moreover, in practice, an ion does not gain much more energy from the web than it does from one off-resonance wave. This is due to the fact that the channels through which an ion could gain a lot of energy become so thin at high energies, that the time needed for such an energization is too long to be practically applicable or observable.

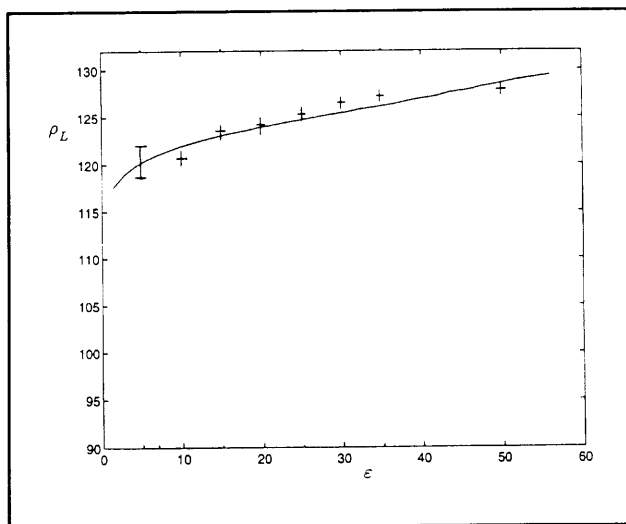


Figure 3. Lower bound of the web ρ_L versus ϵ in the case where $\nu = 140$. The solid line is the analytical result, the pluses are the numerical estimates.

Acceleration of Low Energy Ions

We have shown¹³ both analytically and numerically that an ion acted upon by two waves can be accelerated even if its energy is below the lower bound of the stochastic region. The maximum energy an ion can achieve is nearly independent of its initial energy. The acceleration occurs only if the difference between the wave frequencies is an integer multiple of the ion cyclotron frequency. There is no threshold in amplitude for such an acceleration to

take place, but the time for acceleration is proportional to ϵ^{-2} . The amount of energy a particle receives crucially depends on the ratio between the two wavenumbers. Depending on this ratio, an ion can be coherently accelerated up to the stochastic region where it rapidly gains a lot of energy, or it can gain a more limited amount of energy and remain below the stochastic region, or it can even be decelerated (see figure 4). All of these results can be obtained analytically through a second order perturbation theory performed on the Hamiltonian equation (2). This lets us define an integrable Hamiltonian \tilde{H} whose orbits are very close to the ones obtained by numerically solving the Hamilton equations for equation (2).

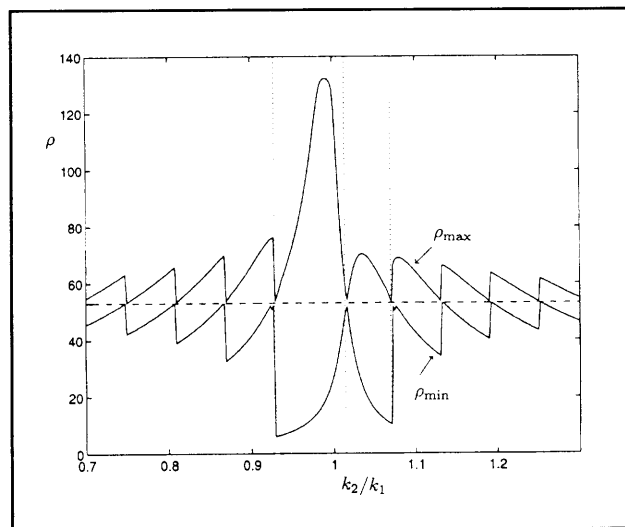


Figure 4. Maximum ρ_{max} and minimum ρ_{min} values of the normalized Larmor radius ρ of a particle versus the ratio of the two wavenumbers. The normalized frequencies of the two waves are $\nu_1 = 140$ and $\nu_2 = 139$. The initial Larmor radius of the particle is $\rho(0) = 53$, and its initial angle is $\theta_0 = \pi/2$.

The perturbation theory also gives good results in the case of more than two waves. As a second order perturbation theory only involves the nonlinear interaction of two waves, the results obtained for two waves are directly applicable to the case of any discrete spectrum of waves. An ion can thus also be coherently accelerated with more than two waves. The difference in the wave frequencies has to be an integer multiple of the ion cyclotron frequency.

¹¹ G.M. Zaslavsky, R.Z. Sagdeev, D.A. Usikov, and A.A. Chernikov, "Weak Chaos and Quasi-Regular Patterns" (Cambridge, England: Cambridge University Press, 1991).

¹² D. Benisti, A.K. Ram, and A. Bers, "Lower Bound in Energy for Chaotic Dynamics of Ions," submitted to *Phys. Lett. A*.

¹³ D. Benisti, A.K. Ram, and A. Bers, manuscript in preparation.

Enhancement of the Maximum Ion Energy

When the initial energy of the ions is close enough to the lower bound of the stochastic region so that it can access the stochastic region, we have found that in the case of two on-resonance waves, the maximum energy it can achieve is much higher than in the case of one wave (see figures 5 and 6). This is due to the existence of structures in phase space which extend to very high values of the action I . These structures are stochastic, but their "skeleton" can also be derived by a first order perturbation expansion of equation (2). Actually, stochasticity plays a negligible role over a wide range of values of the waves' amplitudes. The structures obtained in the case of at least two on-resonance waves are completely different from the web structure existing for one on-resonance wave. In particular, their size is much larger than the size of one cell of the web. This is the reason why they lead to much more acceleration. The acceleration also depends on the ratio of the wavenumbers. For the same amplitudes, and during the same time interval, an ion can gain from three to 90 times more energy than with one wave.

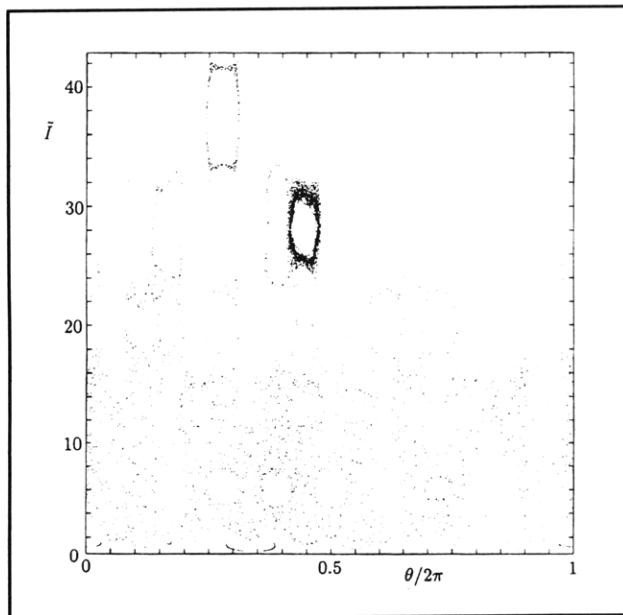


Figure 5. Poincaré surface-of-section of the dynamics of an ion interacting with one wave having a frequency $\nu = 9$ and amplitude $\epsilon = 3.24$ ($\tilde{I} = I/\nu$). The time of integration corresponds to 10,000 cyclotron periods.

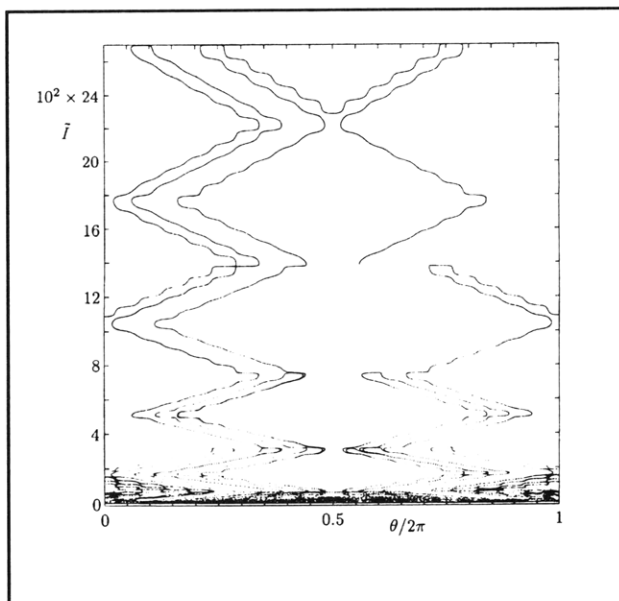


Figure 6. Poincaré surface-of-section of the dynamics of an ion interacting with two waves having frequencies $\nu_1 = 9$ and $\nu_2 = 10$, amplitudes $\epsilon_1 = \epsilon_2 = 3.24$, and with the ratio of the wavenumbers $k_2/k_1 = 0.85$ ($\tilde{I} = I/\nu_1$). The time of integration corresponds to 10,000 cyclotron periods.

This theoretical study has a direct application in providing an explanation for the acceleration of ions in the ionosphere. Since the first discovery of large fluxes of energized ionospheric hydrogen and oxygen ions in the magnetosphere, the terrestrial ionosphere is considered to be a major source of the magnetospheric plasma. The ionospheric ions are collisionally coupled to neutrals in the atmosphere so that the ambient ionospheric temperature is about 0.3 eV. The gravitational escape energies from a 1000 km altitude above the polar region is approximately 0.6 eV for H^+ and approximately 9.6 eV for O^+ . Thus, the first step in explaining the presence of ionospheric ions in the magnetosphere is determining the mechanism whereby the cold ambient ions reach gravitational escape energies. The observations of rockets in the auroral ionosphere seem to associate the presence of accelerated ions to the existence of "spikelets" which are localized regions of an intense electric field. The electric field in the spikelets is composed of electrostatic waves propagating perpendicularly to the geomagnetic field. The observed accelerated ions inside the spikelets have energies of the order of 10 eV. The typical wave frequencies, as well as the thermal energies of the ions, as observed by the rockets, show that the thermal energy of O^+ is much below the bound equation (3). Thus, a stochastic acceleration cannot explain the energization of these ions. Nevertheless, the observed energies for the accelerated ions O^+ can be explained using

the concept of coherent acceleration introduced here.

Moreover, the bound equation (4) corresponds to an energy of 3.6 eV for H⁺ (compared to the observed 10 eV). Hence, the rocket observations for H⁺ can only be explained by using the enhancement of the acceleration in the case of more than one wave, which we described here.

Thus, the theoretical study we performed on the dynamics of multiple waves propagating across a uniform magnetic field seems to yield a basis for understanding the acceleration of ions in the ionosphere.

1.2.3 Interaction of Bootstrap Current and RF Waves in Tokamaks

Sponsors

U.S. Department of Energy
Contract DE-FG02-91-ER-54109

Project Staff

Professor Abraham Bers, Dr. Abhay K. Ram, Dr. Joachim S. Theilhaber, Steven D. Schultz

Work is in progress on the interaction of radio frequency (RF) waves and the bootstrap current in tokamaks. We are continuing to use numerical methods, primarily Fokker-Planck collisional/quasilinear codes, in conjunction with kinetic theory to analyze the velocity-space distribution of electrons.

The current carried by electrons (including bootstrap current) can be found by taking the parallel velocity moment of their distribution function f ,

$$J_{\parallel} = -e \int d^3v v_{\parallel} f. \quad (5)$$

We take f to be at steady state, averaged over the gyromotion, and independent of the toroidal angle ϕ due to axisymmetry. Under these assumptions, f can be written as a function of the guiding center coordinates r and θ and two constants of the motion, the electron's energy E and magnetic

moment μ . Then f satisfies the *drift kinetic equation* (DKE)

$$v_{\parallel} \frac{B_{\theta}}{B} \frac{1}{r} \frac{\partial f}{\partial \theta} + v_{Dr} \frac{\partial f}{\partial r} = C(f) + Q(f). \quad (6)$$

where $C(f)$ is a collision operator, and $Q(f)$ is the quasilinear operator for diffusion due to RF waves.

In an earlier progress report,¹⁴ we described one way of solving equation (6) through expansion in small parameters. The result was

$$f = f_0^{(0)} + \tilde{f}_1^{(0)} + \bar{f}_1^{(0)}. \quad (7)$$

The modified electron distribution due to RF effects only was the solution to

$$\langle C(f_0^{(0)}) + Q(f_0^{(0)}) \rangle = 0 \quad (8)$$

where the brackets indicate averaging over a bounce orbit. Inclusion of guiding center drifts gives

$$\tilde{f}_1^{(0)} = -\frac{m}{eB_0} v_{\parallel} \frac{\partial f_0^{(0)}}{\partial r} \quad (9)$$

and the additional equation

$$\langle C(\bar{f}_1^{(0)}) + Q(\bar{f}_1^{(0)}) \rangle = S \quad (10)$$

with the "source term"

$$S \equiv -\langle C(\tilde{f}_1^{(0)}) + Q(\tilde{f}_1^{(0)}) \rangle. \quad (11)$$

The Fokker-Planck code KT3D has been developed to perform the numerical calculations needed to solve equations (8) and (10). This code is based on numerical methods which have been very successful in RF current drive and electron cyclotron heating theory.¹⁵ KT3D solves for $f_0^{(0)}$ and $\bar{f}_1^{(0)}$ on a uniform grid in velocity space and makes use of finite differencing to calculate derivatives. In the preliminary test runs, we have used a linearized collision operator which includes only electron-ion collisions off a fixed Maxwellian background of ions.

¹⁴ A. Bers, A.K. Ram, C.C. Chow, V. Fuchs, K.P. Chan, S.D. Schultz, and L. Vacca, "Plasma Wave Interactions—RF Heating and Current Generation," *MIT RLE Prog. Rep.* 137: 229-237 (1994).

¹⁵ J. Killeen, G.D. Kerbel, M.G. McCoy, and A.A. Mirin, "Computational Methods for Kinetic Models of Magnetically Confined Plasmas," New York: Springer-Verlag, 1986; Mauel, M.E. "Description of the Fokker-Planck Code Used to Model ECRH of the Constance 2 Plasma," Report No. PFC/RR-82-2, (Cambridge, Massachusetts: MIT Plasma Fusion Center, 1982).

This limited operator is sufficient for bootstrap analysis, since it is the deflection of the electrons' path with respect to the magnetic field which creates the bootstrap current.

The benchmarking of this code has consisted of comparing numerically generated results for Maxwellian plasmas with the analytically derived results from neoclassical theory.¹⁶ This is done prior to the inclusion of the RF quasilinear operator. Figure 7 shows a direct comparison of the bootstrap current J_{\parallel}^{BS} for a Maxwellian plasma as calculated by KT3D and as derived.¹⁶ These results show that KT3D agrees very well with theory, although additional work may be needed to improve its accuracy.

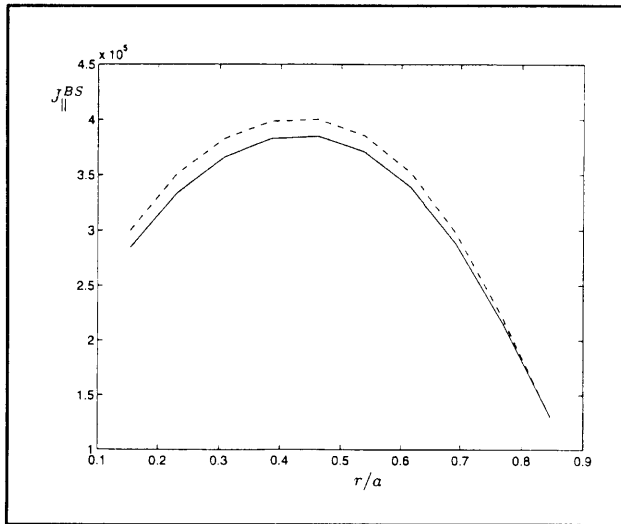


Figure 7. Bootstrap current J_{\parallel}^{BS} for a Maxwellian plasma from KT3D (solid line) and Reference 12 (dashed line).

Once the accuracy of KT3D has been assured, the quasilinear operator will be added in order to calculate the effect of RF waves (lower hybrid, fast Alfvén, electron cyclotron, or ion-Bernstein) on the bootstrap current.

1.2.4 Mode Conversion to Ion-Bernstein Waves of Fast Alfvén Waves With Poloidal Wavenumbers in Sheared Magnetic Fields

Sponsors

U.S. Department of Energy
Contract DE-FG02-91-ER-54109

U.S. Department of Energy
Tokamak Fusion Test Reactor
Contract DE-AC02-78-ET-51013

Project Staff

Professor Abraham Bers, Dr. Abhay K. Ram, Steven D. Schultz

In our previous progress report,¹⁷ the inclusion of poloidal features in the theory of mode conversion of fast Alfvén waves (FAW) at the ion-ion hybrid resonance was first discussed.

We have developed a model in which the mode conversion region is approximately described in a slab geometry by a set of Cartesian coordinates, with the x direction chosen along the equatorial plane of the torus, and the y and z directions corresponding to the poloidal and toroidal directions respectively. The density and magnetic field of the plasma vary only in the x direction. The magnetic field vector lies in the y - z plane, forming an angle $\alpha(x)$ with the z axis. To calculate the dispersion relation for fast Alfvén waves, we rotate the coordinate frame into the direction of the magnetic field, so that at each point x the coordinates must be rotated by $\alpha(x)$. The electric field of the FAW is assumed to have the form

$$\vec{E} = \hat{E}(x) \exp(ik_y y + ik_z z - i\omega t) \quad (12)$$

where k_y and k_z are treated as a constant in the vicinity of the mode conversion region. In the rotated coordinate system the wavenumbers become

$$k_{\parallel} = k_y \sin \alpha + k_z \cos \alpha \quad (13)$$

$$k_{\perp} = k_y \cos \alpha - k_z \sin \alpha. \quad (14)$$

The dispersion relation of the fast Alfvén wave is calculated from cold plasma theory, using the approximation that for a low frequency wave, the electric field in the direction of the equilibrium magnetic field (\hat{E}_{\parallel}) will be shorted out.

The dispersion relation for the FAW gives us a set of two coupled equations for the remaining wave components \hat{E}_x and \hat{E}_z :

¹⁶ M.N. Rosenbluth, R.D. Hazeltine, and F.L. Hinton, *Phys. Fluids* 15: 116 (1972).

¹⁷ A. Bers, A.K. Ram, V. Fuchs, J. Theilhaber, F.W. Galicia, S.D. Schultz, and L. Vacca, "Plasma Wave Interactions—RF Heating and Current Generation," *MIT RLE Prog. Rep.* 138: 247-265 (1995).

$$\frac{d\hat{E}_x}{d\xi} = -\frac{1}{n_x} \left[(D - \psi' n_{\parallel}) \hat{E}_x + i(S - n_x^2 - n_{\parallel}^2) \hat{E}_x \right] \quad (15)$$

$$\frac{d\hat{E}_x}{d\xi} = -\frac{1}{(S - n_{\parallel})}$$

$$\left[i(D' - n_x S + n_x n_{\parallel}^2) \hat{E}_x - (S' - n_x D) \hat{E}_x + i(D - 2\psi' n_{\parallel}) \frac{d\hat{E}_x}{d\xi} \right] \quad (16)$$

In this notation, ξ is once again $(\omega/c)x$, and the primes all indicate differentiation with respect to ξ . S and D are the usual Stix tensor elements.

Studying these equations, we observe that equation (16) is singular at the ion-ion hybrid layer where $S - n_{\parallel}^2 = 0$. \hat{E}_x becomes infinite and resonant absorption occurs. We also observe that if $n_x = 0$, then equation (15) contains a division by zero, and the two equations are no longer coupled. In this case, our analysis is no longer possible, and we are forced to return to the previous mode-conversion theory,¹⁸ which makes use of a single second-order differential equation.

In earlier numerical analyses,¹⁹ there was observed to be significant power loss of the FAW at not only the usual ion-ion hybrid layer but also a second layer where $S - n_{\parallel}^2 - n_x^2 = 0$. However, equations (15) and (16) are not singular at this value, showing that any $S - n_{\parallel}^2 - n_x^2 = 0$ singularity must be removable. Subsequent numerical study has shown that the additional FAW power loss previously discussed can be eliminated by decreasing the plasma collision frequency, leading to the conclusion that this was an added collisional dissipation of the waves and not additional mode conversion.

The numerical integration of equations (15) and (16) is performed with boundary conditions appropriate to total wave reflection at the right-hand FAW cutoff. The region between the cutoff and the ion-ion hybrid resonance then acts as an internal resonator.¹⁸ Figure 8 shows the fraction of power mode-converted for two cases; $k_y = 0$ and $k_y = 8 \text{ m}^{-1}$. The plasma parameters were chosen to fit the features of TFTR during mode-conversion heating experiments. As can be seen, the curves appear similar, but the phase of the internal resonator can be significantly changed by the finite poloidal wavenumber. We notice especially that at low values of k_x (less than 3 m^{-1}), the added

poloidal features give mode-conversion fractions up to 50 percent where there was little mode conversion for $k_y = 0$.

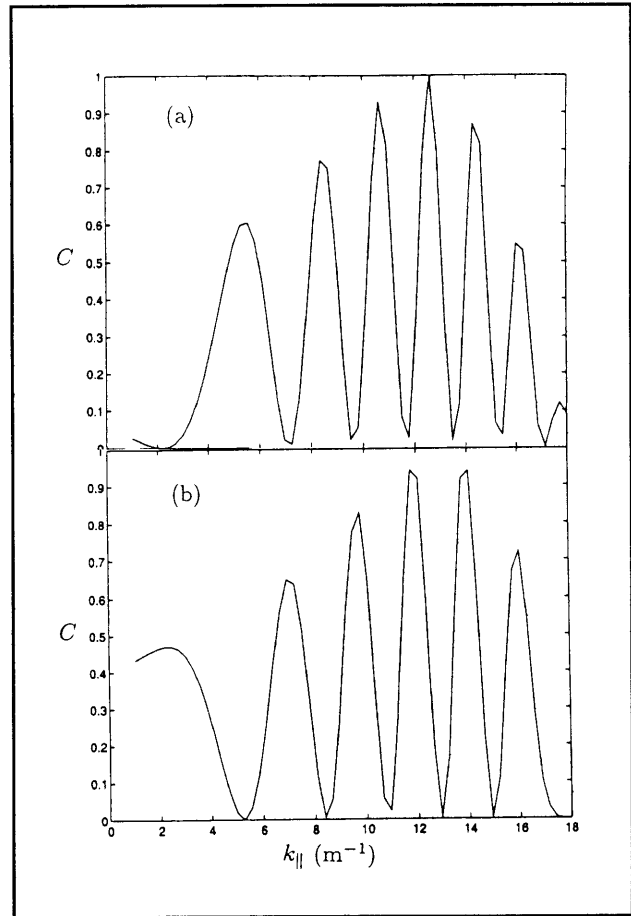


Figure 8. Fraction of FAW power mode-converted (C) as a function of k_{\parallel} for (a) $k_x = 0$ and (b) $k_x = 8 \text{ m}^{-1}$, for a plasma with TFTR parameters.

1.2.5 Current Drive by Mode-Converted Ion-Bernstein Waves

Sponsors

U.S. Department of Energy
Contract DE-FG02-91-ER-54109
U.S. Department of Energy
Tokamak Fusion Test Reactor
Contract DE-AC02-78-ET-51013

¹⁸ A.K. Ram, A. Bers, S.D. Schultz, and V. Fuchs, *Phys. Plasmas* 3: 1976 (1996).

¹⁹ A. Bers, A.K. Ram, V. Fuchs, J. Theilhaber, F.W. Galicia, S.D. Schultz, and L. Vacca, "Plasma Wave Interactions—RF Heating and Current Generation," *MIT RLE Progress Report* 138: 247-265 (1995).

Project Staff

Professor Abraham Bers, Dr. Abhay K. Ram

We have previously studied the propagation and damping of mode-converted ion-Bernstein waves (IBW) in tokamak plasmas heated by radio-frequency waves in the ion-cyclotron range of frequencies (ICRF).²⁰ The IBWs are excited indirectly inside the plasma, near the ion-ion hybrid resonance, when some of the incoming ICRF power, carried by the fast Alfvén waves (FAW), is mode converted to IBWs.²¹ In our previous studies,²⁰ we had shown that if FAWs with $k_{\parallel} \approx 0$ (where k_{\parallel} is the component of the wave vector along the total magnetic field) undergo mode conversion, then it is difficult to generate plasma currents with the IBWs even though the IBWs interacted very efficiently with electrons. This was due to the fact that, before the damping of IBWs, the k_{\parallel} 's tend to shift towards negative values above the equatorial plane and towards positive values below the equatorial plane in a tokamak. Thus, it was difficult to maintain the unidirectionality of the launched FAW spectrum needed for efficient current drive. However, we have recently shown that it is possible to efficiently mode convert FAWs having large values of $|k_{\parallel}|$.²¹ Also, experiments on TFTR have demonstrated current drive by mode-converted IBWs.²² In light of these developments, we have gone back to re-examine the propagation and damping of IBWs when large $|k_{\parallel}|$ can undergo mode conversion.²³ The basic question we have tried to answer is the following: what is the minimum $|k_{\parallel}|$ required at mode conversion so that the unidirectionality of the launched FAW spectrum is maintained as the IBWs propagate and subsequently damp on the electrons?

The results from our previous analysis²⁰ have been very useful in determining the general characteristics of the propagation and damping of IBWs in different plasmas, even though that analysis was for a plasma composed of deuterium ions with a small fraction of hydrogen ions.²⁰ The geometric optics ray trajectory analysis²⁰ shows that $|k_{\parallel}|$ changes rapidly along the IBW rays and that IBWs damp via

electron Landau damping usually near the ion-ion hybrid resonance. The change in k_{\parallel} is given by:

$$\Delta k_{\parallel} \approx -\frac{3\delta}{8} \sin(\theta) \frac{\omega_{cD}}{v_{TD}} \frac{B_{\theta}}{|B|} \frac{|\Delta r|}{R} \quad (17)$$

where θ is the poloidal angle ($\theta = 0$ corresponding to the low-field side), $\delta = \omega/(2\omega_{cD} - \omega)$, ω_{cD} is the deuterium cyclotron frequency, ω is the ICRF frequency, $v_{TD} = \sqrt{kT_D/m_D}$ is the deuterium thermal velocity, B_{θ} is the poloidal magnetic field, B is the total magnetic field, R is the major radius of the tokamak, and Δr is the radial distance of propagation of the ray. From equation (17), we note that the sign of Δk_{\parallel} is negative in the upper half poloidal cross-section of the plasma and positive in the lower half poloidal cross-section. This is the primary effect that can cause the loss of directionality of a launched FAW spectrum. Figure 9a shows the poloidal projection of four IBW rays, with different initial conditions, as they propagate away from the mode-conversion region. The parameters for this simulation correspond to the TFTR experiments.²⁴ The rays are allowed to propagate until they have damped. We note that the IBWs do not propagate very far from the ion-ion hybrid resonance before damping on electrons. Figure 9b shows a magnified view of the four ray trajectories. Since these rays are launched in the upper half poloidal plane, their Δk_{\parallel} should be negative during the propagation. Figures 10a and 10b show that indeed this is the case. However, the rays which were launched with initial values of $k_{\parallel} = 6.5 \text{ m}^{-1}$ do not change their sign of k_{\parallel} before damping. The rays with initial $k_{\parallel} = 6 \text{ m}^{-1}$ change their sign of k_{\parallel} before damping. There are two important points to observe from this simulation. The first point is that if the initial magnitude of k_{\parallel} at mode conversion is large enough, the IBWs propagate and damp on electrons without changing the sign of k_{\parallel} . The second point is that the damping of the IBWs on electrons is localized to being near the mode-conversion region regardless of the k_{\parallel} spectrum. For rays 3 and 4 in figures 9a and 9b, the k_{\parallel} spectrum undergoes a complete reversal of sign over a short distance of propagation (figure 10a). From similar numerical simulations, we have found

²⁰ A.K. Ram and A. Bers, *Phys. Fluids B* 3: 1059 (1991).

²¹ A.K. Ram, A. Bers, S.D. Schultz, and V. Fuchs, *Phys. Plasmas* 3: 1976 (1996).

²² R. Majeski et al., *Phys. Rev. Lett.* 76: 764 (1996).

²³ A.K. Ram and A. Bers, "Current Drive by Mode-Converted Ion-Bernstein Waves." *Bull. Am. Phys. Soc.* 41: 1425 (1996).

²⁴ R. Majeski et al., *Phys. Rev. Lett.* 76: 764 (1996).

that the condition for maintaining a unidirectional spectrum after mode conversion is:

$$\frac{\omega}{|k_{\parallel c}|} \leq 1.3v_{te} \quad (18)$$

where ω is the ICRF frequency, $k_{\parallel c}$ is the value of k_{\parallel} in the mode-conversion region, and v_{te} is the local electron thermal velocity where the IBW is launched. This result depends very crucially on the second point mentioned above.

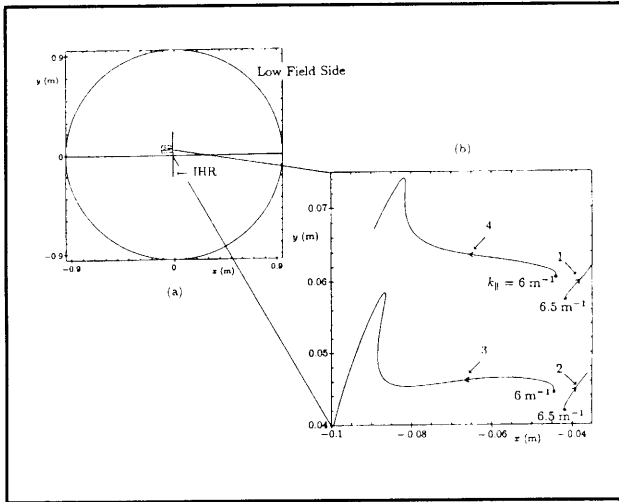


Figure 9. (a) The poloidal projection of the IBW ray trajectories for TFTR-type parameters. The plasma is composed of D-³He-⁴He-C ions with the density ratios of $n_D : n_{^3\text{He}} : n_{^4\text{He}} : n_C = 0.12 : 0.25 : 0.1 : 0.03$. The peak electron density n_0 is $5.5 \times 10^{19} \text{ m}^{-3}$, the peak electron and ion temperatures T_0 are 6.5 keV, the toroidal magnetic field on axis is 4.8 T, the toroidal current is 1.4 MA, the density profile (normalized to the peak density) for the electrons and ions is $0.05 + 0.95(1 - \rho^2)$, and the temperature profile (normalized to the peak temperature) is $0.05 + 0.95(1 - \rho^2)^2$ where $\rho = r/a$ (r is the radial location and $a = 0.95 \text{ m}$ is the minor radius). The major radius is 2.62 m, the ICRF frequency is 43 MHz, and the initial k_{\parallel} 's of the rays are 6.5 m^{-1} (rays 1 and 2) and 6.0 m^{-1} (rays 3 and 4). The approximate location of the ion-ion hybrid resonance is indicated by the line labelled IHR. (b) A magnified view of the ray trajectories shown in figure 9a.

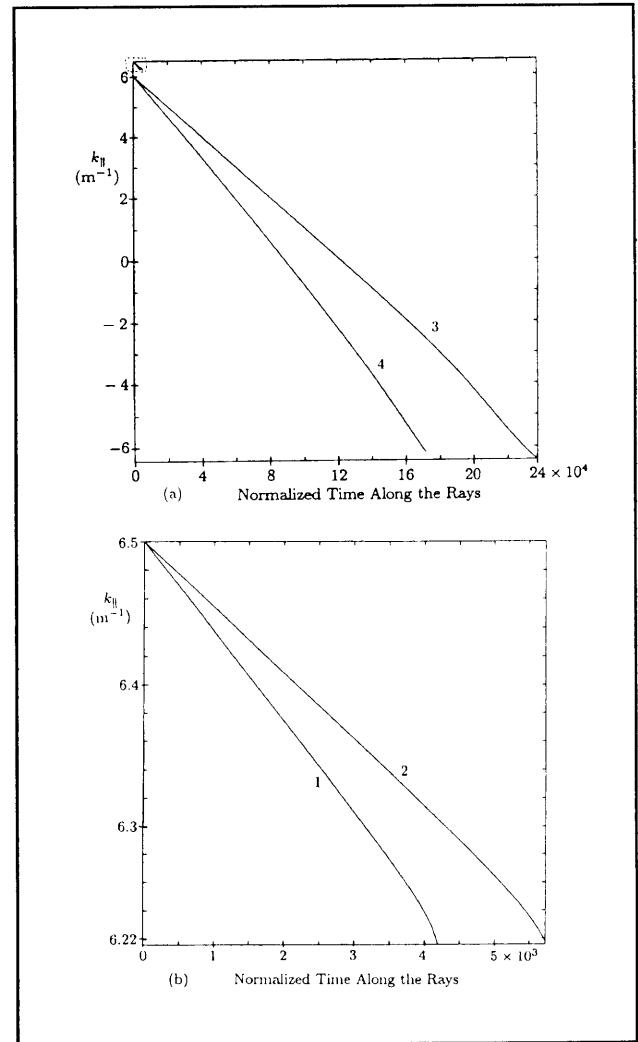


Figure 10. (a) The evolution of k_{\parallel} along the rays of figures 9a and 9b. (b) A magnified view of figure 10a showing the evolution of k_{\parallel} for rays 1 and 2.

The damping of IBWs near the mode-conversion region is an important property which can be used for possible modification of the plasma current profile, e.g., for the reversal of shear near the plasma edge for enhanced plasma confinement. In our previous analysis,²⁵ we found that the radial distance of propagation of an IBW ray for it to electron Landau damp has the following dependencies:

$$\Delta r|_{\text{ELD}} \sim \frac{8}{3\delta} \frac{\omega}{\omega_{cD}} \frac{|B|}{B_{\theta}} \frac{R}{\sin(\theta)} \frac{v_{tD}}{v_{te}}. \quad (19)$$

An important feature of the IBWs emerges from this equation, namely that if the ion and electron tem-

²⁵ A.K. Ram, and A. Bers, *Phys. Fluids B* 3: 1059 (1991).

peratures are the same, the radial distance of propagation depends essentially on the ratio of the ion to electron temperatures. Thus, IBW rays will propagate almost the same radial distance from the mode-conversion region before electron Landau damping whether the region is near the center of the plasma or near the edge of the plasma. This is illustrated in figures 11a and 11b for TFTR parameters where the only change from the parameters in figure 9a is the ICRF frequency; here the frequency is chosen to place the mode-conversion region towards the inside edge of the plasma, into the high magnetic field region. Two IBW rays with initial k_{\parallel} of 6 m^{-1} (ray 1) and 9.9 m^{-1} (ray 2) are launched from near the ion-ion hybrid resonance. Figure 12 shows the corresponding changes in k_{\parallel} as the IBWs propagate away from the mode-conversion region. The k_{\parallel} changes sign for both rays. However, as shown in figure 13, nearly 90 percent of the energy of ray 1 is damped on electrons before k_{\parallel} changes sign. Thus, the initial k_{\parallel} of ray 2 is close to the value for which the entire energy of the IBWs is deposited on electrons without changing the sign of k_{\parallel} . Figures 11a and 11b show that IBWs damp near the mode-conversion region even when this region is moved into the lower temperature part of the plasma. Furthermore, in accordance with the relation in equation (18), the initial k_{\parallel} of the IBW has to be larger, compared to the case of figure 9a where the mode-conversion region was at higher temperatures, so that the IBWs can damp without a change in sign of k_{\parallel} .

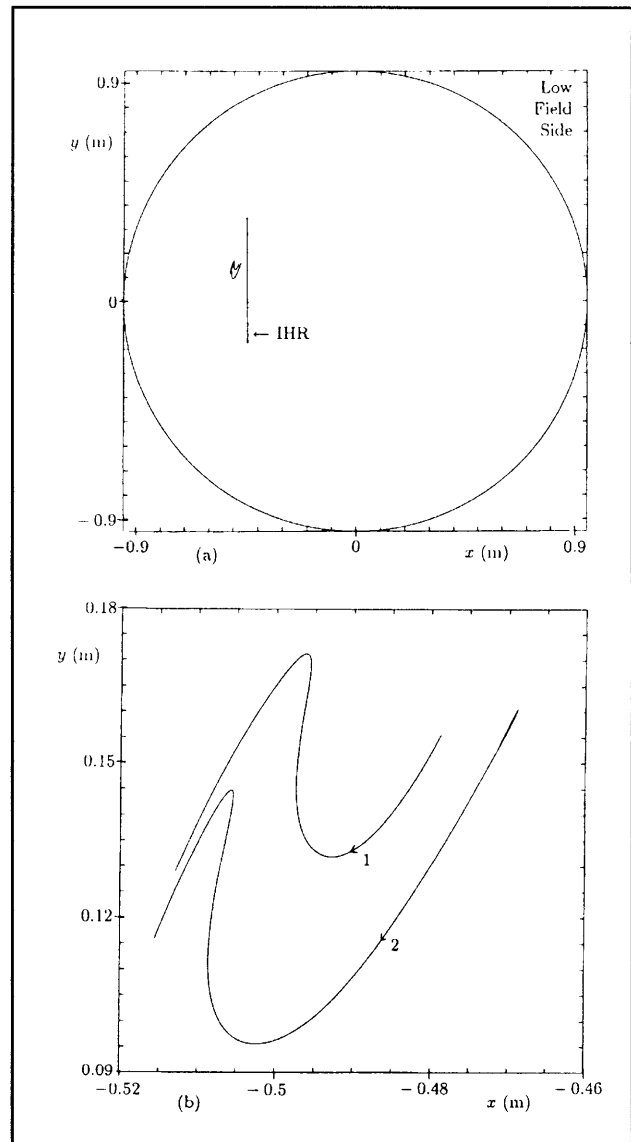


Figure 11. (a) The poloidal projection of two IBW ray trajectories for the same parameters as in figure 9a except that the ICRF frequency is 52 MHz. This places the ion-ion hybrid resonance towards the high-field side (lower temperature region) of the plasma. The two rays have initial k_{\parallel} values of 6 m^{-1} (ray 1) and 9.9 m^{-1} (ray 2). (b) A magnified view of the ray trajectories shown in figure 11a.

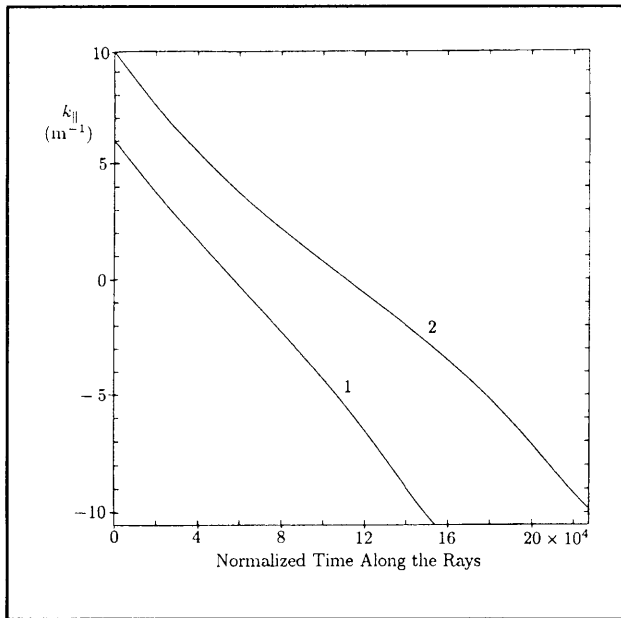


Figure 12. The evolution of $k_{||}$ along the rays of figures 9a and 9b.

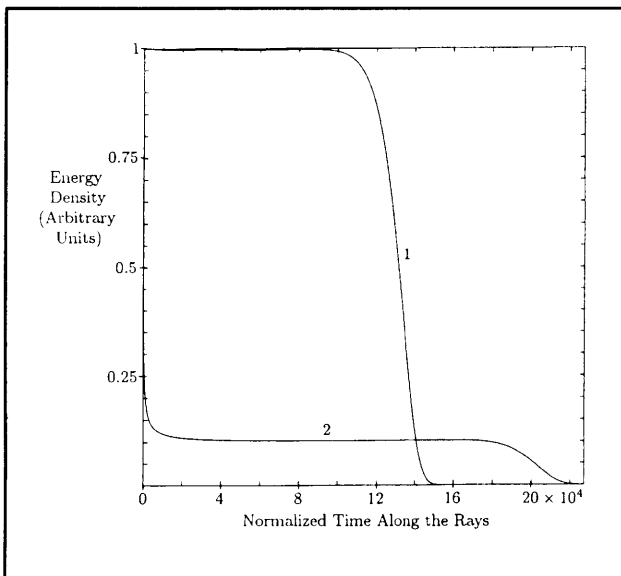


Figure 13. The evolution of the wave energy density along the rays of figures 11a and 11b.

1.2.6 Triplet Mode Conversion from an X-Mode to an Electron Bernstein Wave

Sponsors

U.S. Department of Energy
Contract DE-FG02-91-ER-54109

Project Staff

Professor Abraham Bers, Dr. Abhay K. Ram,
Steven D. Schultz, Kenneth C. Wu

An important way for heating laboratory plasmas is by using radio frequency waves in the electron cyclotron range of frequencies (ECRF). Such waves have been useful for pre-ionization and startup of plasmas, for generation of plasma currents or modifying the current profile, and for controlled plasma heating.²⁶ Substantial progress in the development of gyrotrons has led to this availability of high frequency, long pulsed sources needed for ECRF heating.

In conventional tokamaks (with $\omega_{pe}/\omega_{ce} < 1$, where ω_{pe} and ω_{ce} are the electron plasma and electron cyclotron frequencies, respectively), ECRF waves are typically coupled into the plasma by exciting an ordinary-mode (O-mode) wave polarized with its electric field parallel to the equilibrium magnetic field. The O-mode is absorbed inside the plasma at the electron cyclotron resonance. This means of coupling ECRF waves is not suitable in spherical tokamaks, such as the upcoming National Spherical Tokamak Experiment (NSTX). In spherical tokamaks, $\omega_{pe}/\omega_{ce} \gg 1$ over most of the plasma cross-section and the O-mode is cutoff near the edge of the plasma. We have been studying an alternative method for supplying the ECRF power into the bulk of a spherical tokamak plasma. In this method, the ECRF power is coupled into the plasma by exciting the extraordinary-mode (X-mode) wave polarized with the wave electric field perpendicular to the equilibrium magnetic field. At the upper-hybrid resonance (UHR) located in the plasma, the X-mode undergoes mode conversion to electron-Bernstein waves (EBW), which can then propagate towards the core of the plasma and damp at the electron cyclotron resonance or its harmonics by Doppler-shifted electron cyclotron damping. Simulations of a related mode conversion scheme (O-X-B) have shown that substantial mode conversion can be achieved for a suitable choice of

²⁶ A.C. England and H. Hsuan, "Wave Heating and Current Drive in Plasmas," eds. V.L. Granatstein and P.L. Colestock, (New York: Gordon and Breach, 1985).

ECRF frequencies and parallel wave lengths.²⁷ The mode conversion of the X-mode to the EBW occurs in a region of the plasma where one encounters a cutoff-resonance followed by a cutoff. This is the so-called "triplet" mode conversion scenario, which has been encountered in the ion cyclotron range of frequencies (ICRF), and for which we have provided a complete analytical description.²⁸ In the following, we summarize the triplet mode conversion coefficient for X-mode to EBW. A similar approach to this mode conversion process is alluded to in a paper following the mentioned simulation,²⁹ but details are not given there.

In ICRF heating, a wave in the ion cyclotron range of frequencies is coupled to an ion-Bernstein wave (IBW) at the ion-ion hybrid resonance. Theoretical analysis of this triplet mode conversion process shows that 100 percent mode conversion is possible. We use a similar analysis for the mode conversion of the X-mode to EBW. We assume a cold plasma, with an equilibrium magnetic field in the toroidal direction only, and the ECRF wave propagating in the direction perpendicular to the magnetic field. Using Maxwell's equations, the poloidal component of the wave electric field is given by

$$\frac{d^2 E}{dx^2} + \frac{\omega^2}{c^2} \frac{K_R K_L}{K_L} E = 0. \quad (20)$$

This equation describes the propagation of the X-mode through a resonance ($K_\perp = 0$) and two cutoffs ($K_R = 0$ and $K_L = 0$). This wave equation can be solved analytically as we have shown before.²⁸ We find that the fraction of power mode converted is given by

$$C = 4e^{-\pi\eta}(1 - e^{-\pi\eta})\sin^2\left(\frac{\phi}{2} + \theta\right), \quad (21)$$

where

$$\eta = \frac{\omega_{ce}(x_{UHR})}{\sqrt{2} cb}, \quad (22)$$

and

$$b = \frac{1}{n_e(x_{UHR})} \left| \frac{dn_e(x)}{dx} \right|_{x=x_{UHR}}. \quad (23)$$

θ is the phase of $\Gamma(-i\eta/2)$, ϕ is essentially the phase of the wave reflected from the high-field side left-hand cutoff relative to the incident wave, and x_{UHR} is the position of the upper-hybrid resonance. For substantial mode conversion ($C > 1/2$), one requires typically $0.1 < \eta < 0.5$.

We have applied the above analysis to the parameters for General Atomic's DIII-D tokamak. Figure 14 shows the plot of the mode conversion coefficient η equation (22) for the parameters of a modern tokamak (General Atomic's DIII-D) as a function of the frequency of the excited wave. To achieve the desired range of η for DIII-D requires sources in the frequency range of $42 \text{ GHz} < f < 44 \text{ GHz}$. For all choices that would lead to significant mode conversion, the triplet occurs near the plasma edge. This is due to the fact that for a significant amount of power to be mode converted, it is necessary that the distance between the first cutoff and the resonance (effectively η) be small. As a result, as seen from equations (22) and (23), the density gradient near the resonance must be very steep, and, in general, the density is steepest near the edge of the plasma.

²⁷ S. Nakajima and H. Abe, *Phys. Lett. A* 124: 295 (1987).

²⁸ A.K. Ram, A. Bers, S.D. Schultz, and V. Fuchs, *Phys. Plasmas* 3: 1976 (1996).

²⁹ S. Nakajima and H. Abe, *Phys. Rev. A* 38: 4373 (1988).

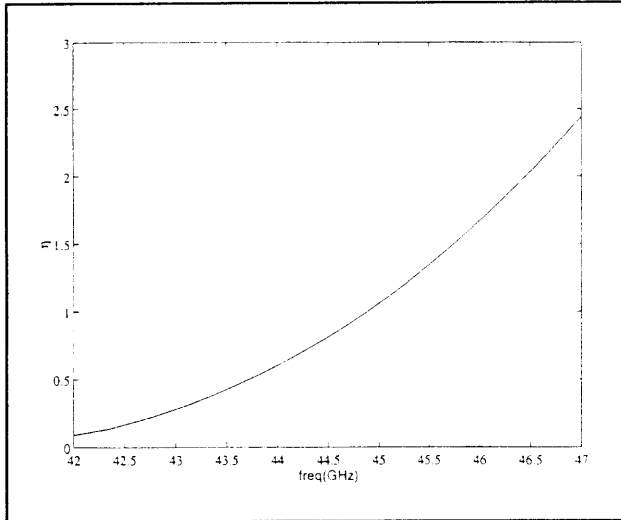


Figure 14. Plot of the mode conversion parameter η as a function of the frequency of the RF wave for DIII-D. Here, $a = 0.7$ m, $R = 1.7$ m, $B_0 = 2$ T and $n_e = n_{\text{edge}} + (n_0 - n_{\text{edge}})[1 - (x/a)^2]^{1/2}$, where $n_{\text{edge}} = 1.6 \times 10^{18} \text{ m}^{-3}$ and $n_0 = 8 \times 10^{19} \text{ m}^{-3}$.

Since both EBWs and electron heating are due to finite electron temperatures of the plasma, we need to consider a Vlasov description to account for them. A wave whose wavevector has a nonzero component in the direction parallel to the equilibrium magnetic field can be damped if its Doppler-shifted frequency, $\omega - k_{\parallel}v_{\parallel}$ where k_{\parallel} and v_{\parallel} are the wavevector and velocity of the particle in the direction parallel to the magnetic field, is equal to a harmonic of the cyclotron frequency. Since this effect is only present when there is a nonzero k_{\parallel} , knowledge of how parallel wavevectors affect wave propagation and mode conversion is crucial. Using our code which numerically solves the hot plasma dispersion relationship, we have studied the propagation and damping of EBWs for typical tokamak

parameters. In figure 15, we plot the hot plasma dispersion relationship near the mode conversion region. In particular, the figure shows the coupling of the X-mode to the Bernstein wave. The mechanism by which the EBW power is delivered to the electrons is through cyclotron damping. Figure 16 shows the propagation and damping of the EBW away from the mode conversion region. Previous analysis has shown that substantial k_{\parallel} will change the nature of the coupling significantly.³⁰ Figure 17 shows how the cold plasma dispersion relation near the edge is affected by varying k_{\parallel} . We are currently trying to understand how nonzero k_{\parallel} will affect our triplet mode conversion scenario.

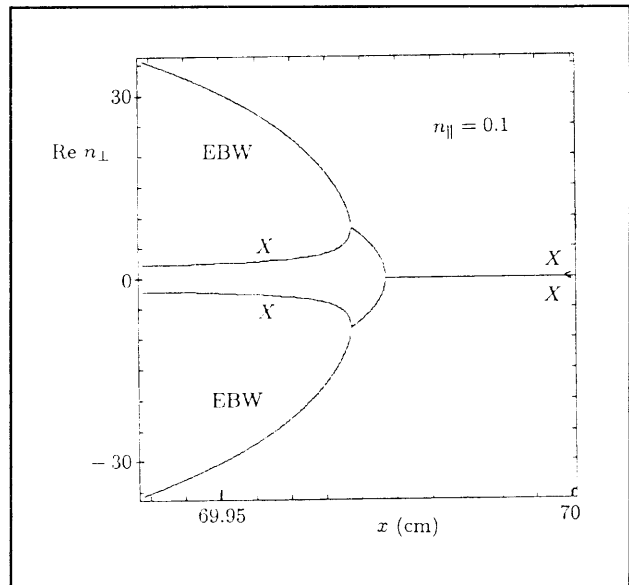


Figure 15. Numerically calculated hot Maxwellian plasma dispersion relation for DIII-D showing the mode conversion of the X-mode wave to an electron-Bernstein wave near the edge. Here, $n_{\perp} = k_{\perp}c/\omega$.

³⁰ J. Preinhaelter and V. Kopecky, *J. Plasma Phys.* 10: 1 (1973).

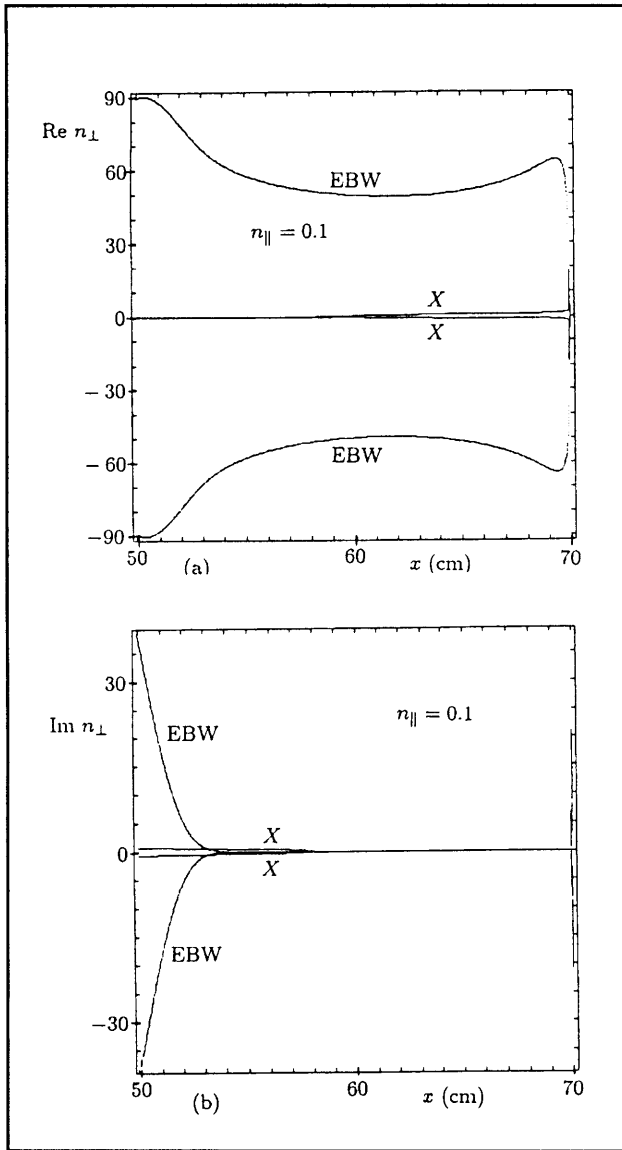


Figure 16. Numerically calculated hot Maxwellian plasma dispersion relation for DIII-D showing the EBW (a) propagating away from the mode conversion region and (b) the damping of the EBW. The damping increases rapidly in the vicinity of $x = 50$ cm, which is where $\omega = \omega_{ce}$.

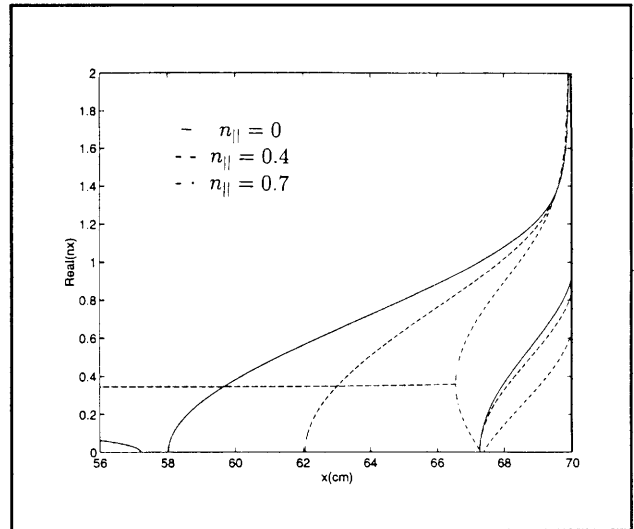


Figure 17. The cold plasma dispersion relationship for DIII-D for waves with different $n_{||} = k_{||}c/\omega$.

In addition to DIII-D, we have also initiated a study of ECRF heating and current drive in NSTX. Unlike conventional tokamaks, the magnitude of the equilibrium poloidal magnetic field in NSTX is of the same order of magnitude as the toroidal field. Figure 18 shows that the triplet mode conversion is also present for NSTX. We are currently assessing the effect of such poloidal magnetic fields on the X-to-EBW mode conversion process.

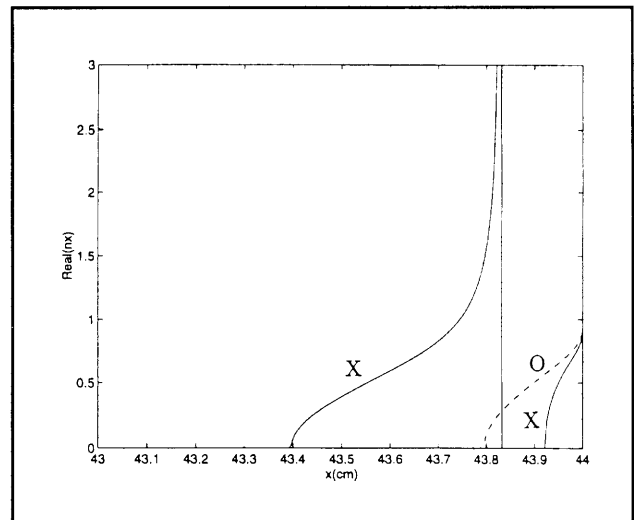


Figure 18. The "triplet" scenario in NSTX calculated from the cold plasma dispersion relationship. Here, $a = 0.44$ m, $R = 0.8$ m, $n_e = n_{edge} + (n_0 - n_{edge})[1 - (x/a)^2]^{1/2}$, where $n_{edge} = 6 \times 10^{17} \text{ m}^{-3}$ and $n_0 = 3 \times 10^{19} \text{ m}^{-3}$. In the region shown, $B_T = 0.22$ T, $B_P = -0.08$ T.

1.2.7 Publications

- Benisti, D., A.K. Ram, and A. Bers. "Coherent Acceleration of Particles by Perpendicularly Propagating Electrostatic Waves." *Bull. Am. Phys. Soc.* 41: 1457 (1996).
- Benisti, D., A. K. Ram, and A. Bers. "Lower Bound in Energy for Chaotic Dynamics of Ions." Submitted to *Phys. Lett. A*.
- Benisti, D. "Origin of Diffusion in Hamiltonian Dynamics." Invited abstract. *Bull. Am. Phys. Soc.* 41: 1478 (1996).
- Benisti, D. "Origin of Diffusion in Hamiltonian Dynamics." Invited paper. *Phys. Plasmas*. Forthcoming.
- Bers, A., A.K. Ram, A. Bécoulet, and B. Saoutic. "Global Resonator in Mode Conversion at the Ion-Ion Hybrid Resonance in Tokamak Plasmas." *Bull. Am. Phys. Soc.* 41: 1425 (1996).
- Lashmore-Davies, C.N., V. Fuchs, A.K. Ram, and A. Bers. "Enhanced Coupling of the Fast Wave to Electrons through Mode Conversion to the Ion Hybrid Wave." Submitted to *Phys. Plasmas*.
- Lashmore-Davies, C.N., V. Fuchs, A.K. Ram, and A. Bers. *Enhanced Coupling of the Fast Wave to Electrons through Mode Conversion to the Ion Hybrid Wave*. Report No. UKAEA FUS 341. Abingdon, England: United Kingdom Atomic Energy Authority/Euratom Fusion Association, 1996.
- Lashmore-Davies, C.N., V. Fuchs, A.K. Ram, and A. Bers. *Enhanced Coupling of the Fast Wave to Electrons through Mode Conversion to the Ion Hybrid Wave*. Report PFC/JA-96-32. Cambridge, Massachusetts: MIT Plasma Science and Fusion Center, 1996.
- Majeski, R., J.H. Rogers, S.H. Batha, A. Bers, R. Budhy, D. Darrow, H.H. Duong, R.K. Fisher, C.B. Forest, E. Fredrickson, B. Grek, K. Hill, J.C. Hosea, D. Ignat, B. LeBlanc, F. Levinton, S.S. Medley, M. Murakami, M.P. Petrov, C.K. Phillips, A. Ram, A.T. Ramsey, G. Schilling, G. Taylor, J.R. Wilson, and M.C. Zarnstorff. "Ion Cyclotron Range of Frequency Experiments in the Tokamak Fusion Test Reactor With Fast Waves and Mode Converted Ion Bernstein Waves." *Phys. Plasmas* 3: 2006 (1996).
- Ram, A.K., and A. Bers. "Current Drive by Mode-Converted Ion-Bernstein Waves." *Bull. Am. Phys. Soc.* 41: 1425 (1996).
- Ram, A.K., A. Bers, S.D. Schultz, and V. Fuchs. "Mode Conversion of Fast Alfvén Waves at the Ion-Ion Hybrid Resonance." *Phys. Plasmas* 3: 1976 (1996).
- Ram, A.K., A. Bers, S.D. Schultz, and V. Fuchs. *Mode Conversion of Fast Alfvén Waves at the Ion-Ion Hybrid Resonance*. Report PFC/JA-96-03. Cambridge, Massachusetts: MIT Plasma Science and Fusion Center, 1996.
- Ram, A.K., D. Benisti, and A. Bers. "Nonlinear Acceleration of Ionospheric Ions by Spectrum of Lower-Hybrid Waves." *Eos* (1996 American Geophysical Union Fall Meeting supplement) 77: F634 (1996).
- Ram, A.K., A. Bers, F.W. Galicia, and D. Benisti. "Transverse Acceleration of Ions in the Auroral Ionosphere by Nonlinear Wave-Particle Interactions." *Eos* (1996 American Geophysical Union Spring Meeting supplement) 77: S249 (1996).
- Ram, A.K., D. Benisti, and A. Bers. "Transverse Acceleration of Ions in the Auroral Ionosphere." *Bull. Am. Phys. Soc.* 41: 1615 (1996).
- Saoutic, B., A. Bécoulet, T. Hutter, D. Fraboulet, A.K. Ram, and A. Bers. "Mode Conversion Heating Experiments on the Tore Supra Tokamak." *Phys. Rev. Lett.* 76: 1647 (1996).
- Saoutic, B., A. Bécoulet, T. Hutter, D. Fraboulet, A.K. Ram, and A. Bers. *Mode Conversion Heating Experiments on the Tore Supra Tokamak*. Report PFC/JA-95-39. Cambridge, Massachusetts: MIT Plasma Science and Fusion Center, 1996.
- Schultz, S.D., A. Bers, and A.K. Ram. "Mode Conversion to Ion-Bernstein Waves of Fast Alfvén Waves With Poloidal Wavenumbers in Sheared Magnetic Fields." *Bull. Am. Phys. Soc.* 41: 1424 (1996).
- Wu, K.C., A.K. Ram, and A. Bers. "Electron Cyclotron Heating and Current Drive in High-Density, Spherical-Type Tokamaks." *Bull. Am. Phys. Soc.* 41: 1425 (1996).

1.3 Physics of High-Energy Plasmas

Sponsor

U.S. Department of Energy
Grant DE-FG02-91ER-54109

Project Staff

Professor Bruno Coppi, Dr. Augusta Airoidi, Dr. Madurja P. Bora, Dr. Giuseppe Bertin, Dr. Francesca Bombarda, Franco Carpignano, Dr. Giovanna Cennachi, William S. Daughton, Darin R. Ernst, Gianmarco Felice, Ming-Hui Kuang, Dmitri Laveder, Dr. Riccardo Maggiore, Dr. Stefano Migliuolo, Peter Ouyang, Dr. Francesco Pegoraro, Gregory E. Penn, Evan Reich, Marco Ricitelli, Caterina Riconda, Dr. Linda E. Sugiyama, George M. Svolos, Dr. Motohiko Tanaka

The primary activities within this research program are (1) the theoretical study of plasmas with high-energy densities in regimes relevant to present-day advanced experiments and (2) the proposal and planning of new experiments capable of producing fusion burning plasmas. The U.S. fusion program has been recently redirected from its emphasis on attempting to develop a viable power producing reactor on the basis of existing knowledge to one supporting basic science and innovative concepts. This redirection brings our group's long-term research program on fundamental physics and its implications for ignition directly into line with the mainstream goals of the new program.

Our group was the first to propose the study of magnetically confined ignition experiments, taking a leading role in the development of their physics and engineering. The Ignitor experiment (shown in figure 19) was the first proposed (1975) that was designed on the basis of the known physics of thermonuclear plasmas and available technology in order to reach ignition regimes. Our group has always recognized the importance of ignition and devoted attention to it before its relevance was universally acknowledged.

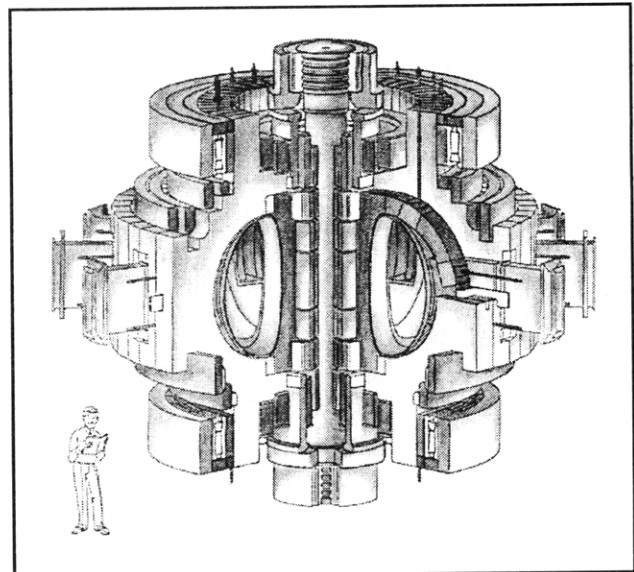


Figure 19. Ignitor Ult machine.

The importance of providing an experimental proof of the process of ignition has recently been underlined³¹ by the Panel on Fusion Research of the President's Committee of Advisors on Science and Technology (PCAST), "Producing an ignited plasma will be a truly notable achievement for mankind and will capture the public's imagination. Resembling a burning star, the ignited plasma will demonstrate a capability with immense potential to improve human well-being. Ignition is analogous to the first airplane flight or the first vacuum-tube computer."

It has become increasingly clear that the most suitable and cost effective type of experiment to pursue the goal of ignition is the line of machines that operate at high-magnetic field, employing cryogenic normal conducting magnets, which we pioneered. These are represented by the series of Alcator machines at MIT and the FT machines at Frascati, Italy, and, specifically intended to study ignition conditions, the Ignitor experiment. A milestone in support of the technological feasibility of this kind of machine is the completion of the construction and testing of full size prototypes of the key components of the Ignitor device. In fact, the ITER design of a large volume D-T burning machine that has been proposed more recently, has been evolving towards an ignition path similar to the one developed for Ignitor. This involves limiting as far as possible the reliance on injected heating, controlling the evolution of the current density profile for reasons of plasma stability, and adopting a similar confinement

³¹ Report to the Fusion Review Panel, President's Committee of Advisors on Science and Technology, O.S.T.P. (Washington, D.C.: White House, 1995).

configuration with the same low aspect ratio and similar structural solutions for the relevant magnet systems. Furthermore, during its design process the limitations of a large scale experiment based on existing superconducting magnet technologies have become more evident. In fact, our view that the technology needed for power-producing fusion reactors should be developed in parallel with the experiments that are needed to investigate physical regimes relevant to fusion burn conditions has now become widely accepted, as evidenced by the PCAST panel conclusions.

At MIT, the Alcator C-Mod experiment combines the favorable features of an elongated plasma cross section with a high-magnetic field to produce high-plasma currents and sustain high-plasma densities. Alcator C-Mod is operating successfully and has again demonstrated the intrinsic ability of high-field compact devices to span a wide range of plasma parameters. This machine has characteristics very similar to a proposed experiment called Megator, which was intended to produce multi-megampere plasma currents by combining high magnetic fields, tight aspect ratios, and elongated plasma cross sections, that we studied and began to propose in the early seventies as a logical evolution of the Alcator program that we had just established at MIT.

Our group has maintained a pioneering role in the physics of high temperature plasmas, contributing original ideas that have been later taken up by others. Of note are the region of second stability for finite pressure plasmas and the method of raising the central q_0 well above unity to access it, the principle of profile consistency of the electron temperature, the degradation of energy confinement by ion temperature gradient driven modes, the isotopic effect, the existence of impurity-driven modes localized at the plasma edge, the stabilization of sawteeth by energetic particles, and the time dependent path to ignition in magnetically confined plasmas.

The ideas concerning transport processes in high temperature plasmas and the fact that it can be nonlocal in nature, as indicated for example by the principle of profile (temperature) consistency that we put forward originally, have been confirmed by different experiments carried out around the world

and form the basis of several widely adopted approaches to the theory of plasma transport.

The theoretical transport model we proposed involved excitation of the so-called toroidal ion temperature gradient driven (ITG) modes, which we found in 1974, and collisionless trapped electron modes, which we also found originally in 1973. This model has been widely accepted and is incorporated in several sophisticated codes that have been used successfully to interpret present experiments that are attracting widespread interest.

We recall that the suggestion that we had made, in the 1980s, to produce peaked plasma density profiles in the Alcator C experiment, in order to avoid the confinement degradation that was afflicting it, originated from the idea that the excitation of ITG modes was its likely cause. The success of the pellet injection experiments, which produced peaked density profiles that led to record values of the confinement parameter $n\tau$ in Alcator, supported the validity of the relevant transport model. We also notice that the enhanced confinement regimes which have been discovered more recently, e.g., by producing a negative magnetic shear configuration, involve the triggering of a state characterized by peaked density profile.³²

We were the first to point out the importance of the so-called "isotopic effect" corresponding to the observation that the confinement time improves³³ as the mass of the hydrogen isotopes, which are the main plasma component, increases. We provided the first theoretical model,³⁴ which has continued to attract strong interest. Consistent with expectations for this theory, the isotopic effect has been found to be present in the transport of angular momentum in rotating plasmas.

The first suggestion to use a divertor to improve the energy confinement was included in a paper by Coppi, Rosenbluth, and Sagdeev in 1976, as a result of the analysis of the properties of the elementary η_i - modes driven by the ion temperature gradient that can be found in a one-dimensional geometry. The same analysis was used as the basis for introducing an effective diffusion coefficient of the thermal energy that has become popular in recent years and is commonly referred to as the "gyro-Bohm" coefficient.

³² F.M. Levington, M.C. Zarnstorff, S.H. Batha, et al., *Phys. Rev. Lett.* 75: 4417 (1995).

³³ B. Coppi, G. Lampis, F. Pegoraro, L. Pieroni, and S. Segre, MIT Report PRR 75/24 (1975).

³⁴ B. Coppi, *Plasma Physics and Controlled Nuclear Fusion* (Vienna: IAEA, 1991) 2: 413 (1990).

There is an increasing body of experimental evidence supporting the elements that characterize the so-called second stability region for finite β plasmas, that we had discovered originally, such as the good confinement characteristics of regimes with vanishing magnetic shear. We have followed closely these developments and those concerning experiments with reversed shear, given their intrinsic value, but also in view of the fact that these regimes can be explored in ignited plasmas by experiments of the Ignitor type.

Internal macroscopic modes that can locally destroy the magnetic field configuration, for which we developed the original theory and analyses, have been recognized by the international community as important potential obstacles to reaching ignition conditions. This is a particularly serious issue for the stated objectives of the ITER project, given the choice of its parameters dictated by the adoption of superconducting magnets. The fields, which this kind of magnet can produce are, in fact, limited to values that do not provide an appropriate margin against the instability of these modes.

The series of experiments with deuterium-tritium plasmas that have been carried out recently has renewed our interest in a series of problems related to the presence of energetic particle populations in magnetically confined, thermal plasmas. Among these we point out that the radiation emission at the harmonics of the ion cyclotron frequency of the fusion products in D-T plasmas finds a consistent explanation³⁵ in the theory of spatially localized modes, that was developed originally by us for spin polarized fusion plasmas.³⁶ The validity of this analysis has been widely verified by now and we are pursuing it farther in view of its potential applications, such as to infer easily the radial distribution of the α -particle population from the spectrum of the relevant emitted radiation, in future D-T burning plasma experiments.

Referring to subjects, in the same general area, that have been popular recently, we mention that an extensive paper concerning the effects of α -particles on ballooning and shear-Alfvén modes was

published in 1981 in *Annals of Physics* by Coppi and Pegoraro.

We have developed and continue to have a strong interest in studying experiments, that can be designed on the basis of present day technologies and can investigate the fusion burning conditions of tritium-poor, nearly pure deuterium plasmas or deuterium-helium 3 plasmas. These experiments are based on combining the main characteristics of high field machines (e.g., Ignitor) with the physics of burning plasmas whose hot core enters the second stability region.

Our analyses of the properties of the plasmas produced by the Alcator C-Mod device has led us to identify salient characteristics, of the physical regimes that have been accessed, which give valuable theoretical insights into the nature of the relevant energy transport processes and are expected to be important for future experiments.

1.3.1 The Ignitor Experiment

We have pursued a long-term project on the design and physics of tight aspect ratio, high magnetic field experiments that are intended to investigate D-T fusion ignition conditions using presently available technology. Our studies³⁷ have shown that the most promising and advantageous ignition designs should rely on an interlocking set of characteristics: tight aspect ratio, relatively small size with significant vertical elongation, high toroidal and poloidal magnetic fields, large plasma currents, high plasma densities, good plasma purity, strong ohmic heating, good plasma and α -particle confinement, and robust stability against ideal MHD and resistive plasma instabilities. These criteria have formed the basis for our design of the Ignitor Ult³⁸ experiment. We note that the ITER design has been evolving, independently, in a similar direction.

The Ignitor ULT machine³⁸ has reached a stage in which the construction³⁹ of full size prototypes of its major components and the testing of key assembly procedures has been completed in Italy. Work is

³⁵ B. Coppi, *Phys. Lett. A* 172: 439 (1993).

³⁶ B. Coppi, S. Cowley, P. Detragiache, R. Kulsrud, and F. Pegoraro, *Phys. Fluids* 29: 4060 (1986).

³⁷ B. Coppi, M. Nassi, and L. Sugiyama, *Phys. Scripta* 45: 112 (1992).

³⁸ B. Coppi, M. Nassi, and L. Sugiyama, *Phys. Scripta* 45: 112 (1992); B. Coppi and the Ignitor Project Group, *J. Fusion Energy* 13: 111 (1994).

³⁹ B. Coppi and the Ignitor Project Group, *J. Fusion Energy* 13: 111 (1994); F. Carpignano, B. Coppi, and M. Nassi, "Prototypes Construction in the Ignitor Program," *Bull. Am. Phys. Soc.* 40:1658 (1995).

proceeding on assembling a complete toroidal sector (1/12th) of the device, on building and testing additional pieces, and on the design of various sub-systems. As a measure of the progress and momentum of the Ignitor project, we note that the last three meetings of the Division of Plasma Physics of the American Physical Society (1994-1996) each had a sub-session devoted to Ignitor, at which a total of 27 presentations were given. The titles of papers presented the past two years give some idea of the scope of the work being carried out by the Ignitor design team.⁴⁰

Recently, we have investigated⁴¹ the possibility of using the enhanced confinement that has been observed to be associated with reversed shear profiles (nonmonotonic current density profiles) in neutral beam heated experiments for ignition in compact experiments. This regime would complement the conventional ignition scenario at high magnetic field and density, since it allows operation at lower current and density. The lower current has the advantage of being easier to maintain for longer periods of time and therefore allows the investigation of longer fusion burning discharges.

As a longer term project, we are continuing to develop a potential design for an advanced fusion experiment that will burn D and ³He, the Candor,⁴² in a combined program of physics and engineering that parallels the Ignitor design for D-T. The pro-

posed design has a similar maximum toroidal field to the Ignitor, in a larger plasma that can support a larger current ($I_p \approx 18\text{-}24$ MA). Normal conducting magnets are envisioned for the toroidal field coils, and a number of the engineering solutions developed for the Ignitor magnets and coils have been adapted for Candor. Numerical simulations, e.g., Coppi and Sugiyama (1988)⁴³ emphasize that the most important property of D-³He ignition is its strong time dependence and dynamic nature, even more so than D-T ignition. A large number of questions remain to be answered in both physics and the engineering design.

1.3.2 Studies of Fusion Ignition Conditions in Magnetically Contained Plasmas

Magnetically confined, toroidal plasmas have reached the stage of development where the detailed analysis of the conditions under which fusion ignition can be achieved must be carried out to design and build the next major experiments.

The regimes under which ignition can be achieved⁴⁴ have a rather well-defined set of characteristics that severely constrain the design parameters. Plasma instabilities driven by the plasma pressure gradient become a concern, since relatively high plasma pressures are required. Projected central plasma pressures range from $p_0 \approx 7.4 \cdot 10^{21}$ keV/m³ for

⁴⁰ F. Carpignano, B. Coppi, and M. Nassi, "Prototypes Construction in the Ignitor Program," *Bull. Am. Phys. Soc.* 40: 1658 (1995); P. Detragiache, F. Bombarda, and B. Coppi, "Recent Results on Confinement: Physics Basis of Ignitor," *Bull. Am. Phys. Soc.* 40: 1657 (1995); A. Airoldi, G. Cenacchi, and B. Coppi, "Enhanced Confinement Conditions and the Ignitor Experiment," *Bull. Am. Phys. Soc.* 40: 1657 (1995); G. Cenacchi, B. Coppi, F. Ferro, and L. Lanzavecchia, "Plasma Evolution Scenarios in the Ignitor-Ult Experiment," *Bull. Am. Phys. Soc.* 40: 1657 (1995); L. Lanzavecchia, B. Coppi, R. Andreani, M. Gasparotto, C. Rita, M. Roccella, G. Dalmut, R. Marabotto, and G. Galasso, "Poloidal Field Coils Design for the Ignitor Ult Experiment," *Bull. Am. Phys. Soc.* 40: 1658 (1995); G. Galasso, L. Lanzavecchia, and J. Rauch, "The Central Solenoid of Ignitor: Design and Manufacturing Aspects of Prototype Coil," *Bull. Am. Phys. Soc.* 40: 1658 (1995). G. Vecchi, R. Maggiore, and M.D. Carter, "A Conceptual Electrical Design Method of the Strap Antennas Applied to the Ignitor Machine," *Bull. Am. Phys. Soc.* 40: 1658 (1995); M. Riccitelli, G. Vecchi, and R. Maggiore, "Coupling Theory for the Strap Antennas Applied to the IGNITOR Machine," *Bull. Am. Phys. Soc.* 40: 1658 (1995); R. Maggiore, G. Vecchi, and T.S. Bigelow, "A Conceptual Electrical Design of A Folded Waveguide Coupler for the IGNITOR Machine," *Bull. Am. Phys. Soc.* 40: 1658 (1995); The Ignitor Project Group and B. Coppi, "Present Context of Fusion Research and the Ignitor Experiment," *Bull. Am. Phys. Soc.* 41: 1488 (1996); G. Cennacchi, A. Airoldi, F. Bombarda, B. Coppi, and J.A. Snipes, "Assessment of Recent Results on Transport and Expectations for Ignitor," *Bull. Am. Phys. Soc.* 41: 1488 (1996); A. Airoldi, G. Cenacchi, and B. Coppi, "Ignition Approach Under L-mode Scaling in Ignitor," *Bull. Am. Phys. Soc.* 41: 1488 (1996); M. Roccella, G. Cenacchi, M. Gasparotto, C. Rita, A. Pizzuto, B. Coppi, and L. Lanzavecchia, "Plasma Engineering in the Ignitor Experiment," *Bull. Am. Phys. Soc.* 41: 1488 (1996); A. Pizzuto, A. Capriccioli, M. Gasparotto, A. Palmieri, C. Rita, M. Roccella, and B. Coppi, "Radial Electromagnetic Press for Ignitor," *Bull. Am. Phys. Soc.* 41: 1488 (1996); C. Ferro and F. Bombarda, "First Wall in the Ignitor Machine," *Bull. Am. Phys. Soc.* 41: 1489 (1996); M. Riccitelli, B. Coppi, C.K. Phillips, R.P. Majeski, J.R. Wilson, D.N. Smithe, and G. Vecchi, "ICRF Heating Scenarios for the Ignitor Machine," *Bull. Am. Phys. Soc.* 41: 1489 (1996); R. Maggiore, G. Vecchi, M. Riccitelli, and M.D. Carter, "Electrical Design of an ICRF System for Ignitor," *Bull. Am. Phys. Soc.* 41: 1489 (1996); M.H. Kuang and L.E. Sugiyama, "Reversed Shear Ignition Regimes for High Field Tokamaks," *Bull. Am. Phys. Soc.* 41: 1489 (1996).

⁴¹ L.E. Sugiyama, "Reversed Shear Ignition for High Field Tokamaks," *Proceedings of the European Physical Society Meeting*, Kiev, Ukraine, 1996.

⁴² B. Coppi, *Physica Scripta* T2: 2, 592 (1982); B. Coppi, *Nucl. Instr. Meth. Phys. Res.* A271: 2 (1988).

⁴³ B. Coppi and L.E. Sugiyama, "Questions in Advanced Fuel Fusion," MIT Report RLE PTP-88/6 (1988).

⁴⁴ B. Coppi, L. E. Sugiyama, and M. Nassi, *Physica Scripta* 45: 112 (1992), and references therein.

ITER,⁴⁵ to $p_0 \approx 2.4 \cdot 10^{22}$ keV/m³ for Ignitor.⁴⁴ Confinement at these pressures requires a relatively strong poloidal magnetic field, \bar{B}_p . For this reason and in order to ensure the attainment of the required values of the confinement parameter, $n\tau_E$, where τ_E is the energy confinement time, these devices have been designed to produce high plasma currents.

We maintain an active program of research into the characteristics of both types of experiments. One area of great importance to confinement is the stability of MHD modes. Pressure-driven global "internal" modes⁴⁶ can induce sharp, periodic drops of the central plasma pressure, making ignition difficult or impossible to achieve over reasonable time intervals. In addition, loss of the fusion plasma heating in the center of the plasma column can ensue, as the fast, several MeV, fusion-produced α -particles are expelled by the instability before they can slow down in the plasma. Expulsion of fast particles by sawtooth crashes have been observed experimentally.

By virtue of the fact that Ignitor is a low- β_p experiment in which the region with the magnetic field parameter $q(r) \leq 1$, which is most affected by these modes, is either nonexistent or very small, this experiment is deemed to be relatively insensitive to the consequences of global internal $n=1$ modes (here n is the toroidal mode number). It is well known that these instabilities⁴⁶ are dominated by the $m=1$ poloidal harmonic but also couple to the $m=0,2$ components. The $m=2$ harmonic extends to the $q=2$ surface, which in the case of the ITER reference plasma with an edge $q_a \approx 3.0$, lies at three quarters of the plasma radius, while the $q=1$ surface encompasses fully half the radius.

Our analysis of the linear ideal MHD stability of ITER plasmas shows that, if the design reference pressure and current profiles are assumed, $n=1$ global internal modes will have rather large growth rates. These growth rates are high enough to be unaffected by finite ion Larmor radius and such that the fast alpha particle population will not contribute to stability. By modifying the q -profile to increase the local value of the magnetic shear, the growth rate of the instability can be mitigated but not reduced to the point of being meaningless. Dras-

tically flattening the pressure profile within the $q \leq 1$ region can bring about stabilization of the $m=1$ component (e.g., $p \propto (1-\psi^3)^{3/2}$, where ψ is a normalized magnetic flux coordinate). For ITER there is also the question of whether the reference design parameters, in particular the large toroidal magnetic field of 13.5 T at the coils on the inside of the torus, can in fact be achieved.

The role played by fusion α -particles on the stability of these global modes has been considered briefly. Suprathermal particles can act as an "anchor" for the plasma and stabilize internal modes when the growth rates are relatively mild. Stabilization requires that the relevant plasma parameters (λ_H , ω_i , n_α/n) lie within a finite domain where λ_H is the ideal-MHD stability parameter,⁴⁶ ω_i is the ion diamagnetic frequency, and n_α/n is the α -particle concentration. In the case of the ITER reference operating regime, $\lambda_H \gg \omega_i/\omega_{A0}$, and the α -particle pressure is strong enough to generate its own version of a fluid-like $m=1$ instability.⁴⁷

1.3.3 Excitation of Sawtooth Oscillations in the Alcator C-Mod Experiment

The Alcator C-Mod machine has been in operation for several years at MIT. Its goals include studying the physics of advanced plasma regimes, determining the efficiency of injected RF heating in high plasma densities, and developing and optimizing the design of divertors. It has many of the characteristics of planned ignition experiments, such as plasma shaping, well thermalized plasmas, high power densities, and the ability to explore a relatively wide range of regimes.

In collaboration with the Alcator group, we are engaged in a general study of instabilities in Alcator C-Mod. The first part involves the characterization of sawtooth activity as a function of plasma parameters (i.e., density, temperatures, current, magnetic field, additional heating power). Sawteeth, with very few exceptions, are always present in the plasmas produced by this machine, their period is fairly independent of density, and the period increases as additional RF heating is applied. The amplitude, on the other hand, tends to saturate as

⁴⁵ M.N. Rosenbluth, J. Hogan, D. Boucher, P. Barabaschi, A. Bondeson, B. Coppi, L. Degtyarev, S. Haney, H. Goedbloed, T.C. Hender, H. Holtjes, G. Huysmanns, W. Kerner, J. Manickam, A. Martynov, S. Medvedev, D. Monticello, T. Ozeki, L.D. Pearlstein, F. Perkins, A. Pletzer, F. Porcelli, P.H. Rebut, S. Tokuda, A. Turnbull, L. Villard, and J. Wesley, in *Plasma Physics and Controlled Nuclear Fusion Research 1994* (Vienna: IAEA, 1995), paper CN-60/E-P-2.

⁴⁶ A.C. Coppi and B. Coppi, *Nucl. Fus.* 32: 205 (1992).

⁴⁷ L. Chen, R.B. White, and M.N. Rosenbluth, *Phys. Rev. Lett.* 52: 1122 (1984).

the period increases. Precursor $m=1$ oscillations appear in the last case.

At low density, $\bar{n}_e \approx 0.7 \times 10^{20} \text{ m}^{-3}$, the regular sawtooth activity is sometimes reduced to a different type of oscillation, considerably smaller and more frequent, nearly sinusoidal in shape and radially out-of-phase, and localized in a narrow central region well inside the $q=1$ surface. The frequency is of the order of 1 kHz, to be compared with a repetition period of 5 to 25 msec for the standard sawtooth. Possible causes of this phenomenon are being investigated.

We have assembled a small database emphasizing the physics of sawtooth oscillations and the associated $n=m=1$ precursors. We are engaged in identifying the plasma regimes in which these oscillations develop and comparing the observations with the known linear stability theories. Of the two dozen time points in the database so far, the large majority appear to correlate with the excitation of collisional reconnecting modes,⁴⁸ three are sawtooth-free, and two, in high power, relatively high- β_p , RF discharges, may result from the excitation of ideal MHD modes.

1.3.4 Energy Confinement and Thermal Transport

High-field, compact experiments have a well demonstrated ability to produce a relatively large variety of plasma regimes. We are studying extensively the global confinement of the plasmas produced by the Alcator C-Mod machine. This includes a comparison with the FT machine (Frascati, Italy) which is the only other high-field device presently in operation.⁴⁹ The results from these machines are

especially significant to assess the expected performances of the Ignitor experiment.⁵⁰

The transport analysis has so far evolved along two lines. One is a parametric study of global parameters, such as the energy confinement time, over a large number of discharges, to locate global trends.⁵¹ Recent results have confirmed the positive effect on confinement played by the high currents associated with the plasma vertical elongation. The other line involves the detailed simulation of a relatively small number of discharges over a large range of plasma parameters using a single form of transport coefficient.⁵²

The observed similarity in the global thermal confinement between the ohmic and ICRF heated L-mode plasmas in Alcator C-Mod opens the possibility that thermal transport may be described by one transport coefficient for both regimes. A modified form of a transport coefficient previously proposed⁵² to reproduce the measured profiles for ohmic plasmas has been used to simulate both ohmic and ICRF discharges over a wide range of parameters. In fact, detailed simulations carried out by means of the BALDUR code reproduce rather well the observed temperature profiles, loop voltage and energy confinement time. The coefficient $D_{\parallel}^{\text{th}}$ includes the constraint of profile consistency and is inspired by the properties of the so-called "ubiquitous" modes⁵³ (commonly called collisionless trapped electron and ITG toroidal modes) that can be excited in the presence of a significant fraction of trapped electrons. Thus $D_{\parallel}^{\text{th}}$ includes a significant dependence on the electron pressure gradient. The resulting confinement time improves with the plasma current, in agreement with the observations, and contains only a weak dependence on density. In particular, the coefficient is of the form

⁴⁸ B. Coppi, R. Galvão, R. Pellat, M.N. Rosenbluth, and P.H. Rutherford, *Sov. J. Plasma Phys.* 2:533 (1976).

⁴⁹ F. Bombarda, B. Coppi, W. Daughton, L. Sugiyama, M. Greenwald, A. Hubbard, J. Irby, C. Fiore, J.E. Rice, S. Wolfe, S. Golovato, and Y. Takase, International Sherwood Theory Conference, Incline Village, Nevada, 1995, paper 2D25; F. Bombarda, B. Coppi, W. Daughton, L. Sugiyama, C. Fiore, S. Golovato, M. Graf, M. Greenwald, A. Hubbard, J. Irby, B. LaBombard, E. Marmor, M. Porkolab, J.E. Rice, Y. Takase, and S. Wolfe, *Proceedings of the 22nd European Physical Society Conference on Controlled Fusion and Plasma Physics*, Bournemouth, United Kingdom, 1995, 19C III, p. 17.

⁵⁰ P. Detragiache, F. Bombarda, and B. Coppi, "Recent Results on Confinement: Physics Basis of Ignitor," *Bull. Am. Phys. Soc.* 40: 1657 (1995).

⁵¹ F. Bombarda, B. Coppi, C. Fiore, S. Golovato, M. Greenwald, A. Hubbard, J. Irby, E. Marmor, M. Porkolab, J.E. Rice, Y. Takase, and S. Wolfe, *Bull. Am. Phys. Soc.* 40: 1699 (1995).

⁵² B. Coppi, L. Sugiyama, M. Greenwald, W. Daughton, A. Hubbard, J. Irby, C. Fiore, T. Luke, J. Rice, E. Marmor, S. Wolfe, and R. Granetz, *Proceedings of the 21st EPS Conference on Contributions to Fusion and Plasma Physics, Montpellier, Vermont, 1994, 18B III, p. 520.*

⁵³ B. Coppi and G. Rewoldt, *Phys. Rev. Lett.* 33: 1320 (1974); B. Coppi and F. Pegoraro, *Nucl. Fusion* 17: 963 (1977).

$$D_e^{\text{th}} \propto \left(\omega_{\text{pi}} \frac{c^2 v_{\text{ee}}}{\omega_{\text{pe}}^2 V_{\text{the}}^2} \right)^{2/5} \frac{I}{\text{enR}} \left[\frac{C_1 \beta_{\text{pe}}^*}{q_e^{2/3}} - 1 \right]$$

where $\beta_{\text{pe}}^* = 8\pi p_e' / \langle B_{\theta}^2 \rangle \propto p_e' / I_p^2$ and $p_e' = (dp_e/dr)_{\text{max}} a$ and C_1 is a numerical coefficient ≈ 16 . Both the experimental observations and the simulations indicate that $\beta_{\text{pe}}^*/q_e^{2/3}$ is roughly constant for ohmic discharges while it increases with $(P_H/I_p V_o)$ for ICRF discharges, where P_H is the total heating power and V_o is a characteristic voltage scale ≈ 1 volt. Thus a natural transition between the ohmic and ICRF regimes is included in the coefficient through the pressure gradient dependence. A total of nearly two dozen ohmic and ICRF discharges covering a wide range of the parameter space have been reproduced quite well by this coefficient.⁵⁴

1.3.5 Emission above the Ion Cyclotron Frequency Induced by Fusion Products

In recent years, experiments have for the first time used Deuterium-Tritium mixtures in advanced plasma experiments, with the JET and TFTR machines.⁵⁵ These experiments produce a significant fraction of high-energy particles in the MeV range. The unique properties of these plasmas yield insights into the physical processes that will affect future ignition experiments. In these experiments, enhanced emission at the harmonics of the ion cyclotron frequency of the fusion products has been observed.⁵⁶ In fact, this radiation is strongly correlated with the neutron flux. The theory that we have developed⁵⁷ and that is based on the previous discovery of "contained modes"⁵⁸ is consistent and indicates that significant information about the the

fusion product population distribution, both in velocity space and over the plasma cross section, can be extracted from these observations.

Our model explains the main characteristics of the observed emission, in particular the fact that the radiation peaks occur at frequencies corresponding to harmonics of the α (or D) cyclotron frequency, Ω_α , at the outer edge of the plasma column⁵⁹ (where the B field is considerably lower than that at the center). Our results also indicate a transition from discrete harmonics to a continuum spectrum⁶⁰ at high frequencies that is consistent with observations in the JET experiments⁶¹ of a continuum spectrum for frequencies $\omega \geq 7 \Omega_\alpha$.

In this model, the radiation is the result of the excitation of radially "contained" modes⁶² which are driven unstable by the fusion products at frequencies which are harmonics of the corresponding cyclotron frequency. The spatial variation of the plasma density and the effects of magnetic shear are key ingredients in this theory. The contained modes are solutions of the ideal MHD equations, extended to include the Hall term. Thus, the frozen-in law is replaced by the more general Ohm's equation $\vec{E} + \vec{v} \times \vec{B} = (1/\text{en}) \vec{J} \times \vec{B}$. We focus on quasi-flute modes, whose direction of propagation is mostly perpendicular to the magnetic field, but also has a small component parallel to the magnetic field. These modes are generalizations, to the case of an inhomogeneous plasma, of the magnetosonic-whistler modes⁶⁰ with dispersion relation $\omega^2 = k_\perp^2 (v_A^2 + k_\perp^2 D_w^2)$, where $v_A = B/\sqrt{\mu_0 n m_i}$ is the Alfvén velocity and where we define $D_w = B/\mu_0 n e$. We restrict our attention to modes with a high poloidal number, since we are interested in modes having frequencies $\omega \geq \Omega_\alpha \gg v_A/a$,

⁵⁴ M. Pravia, B. Coppi, W. Daughton, L. Sugiyama, F. Bombarda, and M. Greenwald, *Bull. Am. Phys. Soc.* 40: 1699 (1995); W. Daughton, B. Coppi, F. Bombarda, L. Sugiyama, M. Greenwald, and Alcator-C-Mod, "A Thermal Transport Coefficient for Ohmic and ICRF Plasmas in Alcator C-Mod," *Proceedings of the International Sherwood Fusion Theory Conference, Philadelphia, Pennsylvania, March 18-20, 1996, paper 1D50*.

⁵⁵ G. A. Cottrell et al., *Nucl. Fusion* 33: 1365 (1993); S. Cauffman and R. Majeski, *Rev. Sci. Instrum.* 66: 817 (1995).

⁵⁶ G. A. Cottrell et al., *Nucl. Fusion* 33: 1365 (1993); S. Cauffman, R. Majeski, *Rev. Sci. Instrum.* 66: 817 (1995); JET Team, *Phys. Fluids B* 5: 3 (1993).

⁵⁷ JET Team, *Phys. Fluids B* 5: 3 (1993); B. Coppi, *Phys. Lett. A* 172: 439 (1993).

⁵⁸ B. Coppi, S. Cowley, R. Kulsrud, P. Detragiache, and F. Pegoraro, *Phys. Fluids* 29: 4060 (1986).

⁵⁹ S. Cauffman and R. Majeski, *Rev. Sci. Instrum.* 66: 817 (1995); B. Coppi, *Fusion Technol.* 25: 326 (1994).

⁶⁰ B. Coppi, in *Physics of High Energy Particles in Toroidal Systems*, eds. T. Tajima and M. Okamoto (New York: AIP, 1994); *AIP Conference Proceedings* 311: 47 (1993).

⁶¹ G.A. Cottrell et al., *Nucl. Fusion* 33: 1365 (1993); B. Coppi, *Fusion Technology* 25: 326 (1994).

⁶² B. Coppi, S. Cowley, R. Kulsrud, P. Detragiache, and F. Pegoraro, *Phys. Fluids* 29: 4060 (1986).

where v_A/a is the typical frequency scale for magnetosonic modes. The contained mode can be approximated by taking the limit of cylindrical geometry, which ignores small corrections on the order of the inverse aspect ratio (r/R_0).

We find two qualitatively different solutions for the modes under consideration, occurring in different frequency ranges, as is consistent with the observed spectrum, which has a discrete and a continuum part. The modes corresponding to the discrete spectrum at lower harmonics⁶³ are localized within a narrow, radially localized shell near the plasma edge. The peaks of the discrete spectrum correspond closely to harmonics of the cyclotron frequency at the outboard side of this shell, farthest from the axis of symmetry. For low values of the harmonic number, we find that the mode is always localized about the same radius r_0 . An analysis of the mode solutions reveals that for higher frequency modes, the parallel component of the propagation of the fields causes an increasing shift in the mode localization away from r_0 . These high frequency modes can extend much further radially into the plasma column.⁶⁴ The considerable variation of the magnetic field, and therefore of the cyclotron frequency, over this wide interval implies that the excited modes can have overlapping bands of resonant frequencies.

For the higher harmonics, we find that the change in localization of the mode alone can cause different harmonics of the cyclotron frequency to overlap above a particular harmonic resonance ℓ_{crit} , which is proportional to the aspect ratio of the experiment and also depends on the profiles of the plasma. For $\ell > \ell_{\text{crit}}$, the interval over which modes can be excited extends toward the center of the plasma column, so that more α - particles can interact with the mode. Thus the discrete part of the spectrum yields information specifically about the trapped, energetic particles with large orbits that extend beyond r_0 , while the continuum spectrum can give information about the average density of energetic particles inside the plasma column. Including the effect of other terms in the resonance condition results in the extension of the continuum part of the spectrum so the transition to continuum occurs for a smaller value of ℓ_{crit} .

The radial containment is a fundamental characteristic of our model, since only standing modes can generate sufficient growth of the mode to justify the detected emission power levels. For the type of mode under consideration, the instability evolves on a time scale $1/\gamma$ that is much longer than the typical transit time a/v_A of a mode with radial propagation. This indicates that traveling waves in the radial direction, that would be obtained from a theory for a homogeneous plasma, cannot reach sufficient amplitudes (in view of the convection associated with them and of the weak growth rates that are found) to explain the observed rate of radiation emission.

The distribution function for the interacting particles, which are trapped particles near the outer edge of the plasma, can be described as strongly anisotropic in velocity space and having energies close to their value at birth from the fusion reaction. Sufficiently strong anisotropy will have an important effect on the instability of the mode.

The growth rate can be evaluated using a full toroidal calculation for the particle dynamics, while keeping the "cylindrical" approximation to evaluate the features of the contained mode. The growth rate depends linearly on the α -particle density, and can be of the order of the bounce frequency of the interacting α -particles.

1.3.6 Two-Fluid Models of Plasmas

The stability of macroscopic, low mode number instabilities in high-temperature toroidal plasmas is usually studied using single-fluid MHD, because it has been the only model available that can take into account all the toroidal and 3D effects that are important in tight aspect ratio plasmas. However, it is theoretically inappropriate for many cases to which it is applied and fails to explain many features of present day plasmas that are crucial to their stability and confinement. In this light, we have developed⁶⁵ a fully nonlinear model for the two-fluid plasma (electrons and ions) in a 3D torus without any geometric approximation. This work is part of an ongoing collaboration with W. Park and

⁶³ JET Team, *Phys. Fluids* B5: 3 (1993).

⁶⁴ B. Coppi, *Phys. Lett. A* 172: 439 (1993).

⁶⁵ L.E. Sugiyama and W. Park, *Two-Fluid 3D Model for Toroidal Plasmas*, MIT RLE Report PTP-96/2, in preparation (1997); W. Park, G.Y. Fu, D. Monticello, N. Pomphrey, H. Strauss, and L. Sugiyama, *Bull. Am. Phys. Soc.* 39: 1725 (1994); L.E. Sugiyama and W. Park, International Sherwood Fusion Theory Meeting 1995, Incline Village, Nevada, April 1995, paper 1C13; L.E. Sugiyama, "3D Two-Fluid Simulation of Tokamak Plasmas," invited paper, American Physical Society Division of Plasma Physics Meeting, 1996; *Bull. Am. Phys. Soc.* 41: 1584 (1996).

co-workers at Princeton Plasma Physics Laboratory, Princeton, New Jersey, New York University, and others. The whole M3D project⁶⁶ aims to gradually develop a "comprehensive" numerical model of a magnetically confined plasma. The original model was a fully 3D, toroidal resistive MHD (single fluid) code, to which has been added a gyrokinetic hot particle population. An unstructured mesh spatial grid is also under development, while we have concentrated on adding the effects of the electrons. One advantage of this approach is that effects can be successively turned "on" or "off" by simple changes in the input file to isolate important phenomena and to gain physical insight. This includes the possibility of a simple reduction of the geometry from toroidal to cylindrical, which greatly reduces both numerical and actual complexity.

A two-fluid model is much more complex than a single fluid one, since it picks up a number of additional plasma waves and instabilities that have time and space scales that are much faster and smaller than the main MHD ones, due to the electron involvement. The present model contains the major two-fluid effects, i.e., the ion gyroviscous stress tensor, the Hall and electron pressure gradient terms in the Ohm's law, and the diamagnetic drifts, and electron pressure and density equations. Although the physics remains basically collisional, fundamental kinetic effects appear and a large range of phenomena beyond MHD can be studied. Previous numerical models used to study diamagnetic effects have relied on an aspect ratio expansion or the isothermal approximation, or both. In addition, the standard analytic two-fluid models (e.g., the "drift" approximation, or various reductions of neoclassical MHD) were derived for linearized perturbations. The present model is intended⁶⁷ to extend to the nonlinear evolution in a form which is analytically simple enough to be computationally feasible, yet contains the essential physics. One advantage of the approach based on the keeping the full geometrical effects is that the two-fluid parts

of the model can be fine-tuned after the basic model is working, since this involves more accurate approximations to only a few terms in the equations (the highest order velocity moments). In addition, our investigations show that a number of important effects that are not explicitly in the drift, or conventional two-fluid equations must be included to have a self-consistent nonlinear model. This remains an active area of investigation.

The model has been benchmarked against analytic solution of the dispersion relation for the $m=1$, $n=1$ mode, in the linearized perturbation.⁶⁸ In the process, a simple physical and geometrical interpretation for the stabilization of the mode with increasing ω_i has been found.⁶⁹ The code works stably in both cylinder and torus, even in the fully nonlinear phase. Growth and rotation of magnetic islands formed by (resistive) reconnection has been followed in cylinder and torus. A number of important differences have been found for the torus⁶⁷ compared to the existing theory and to the cylinder (most theories have been worked out for cylindrical or close-to-cylindrical cases).

We plan use the fully toroidal MH3D-T two-fluid model to study a number of instabilities that are now investigated only with MHD. These include most of the "strong," or large scale, instabilities that are experienced by high temperature plasmas, including magnetic islands, coupling to other instabilities, sawteeth, and disruptions.

A major current area of interest is the effect of plasma rotation, both background and instability-driven, on both linear perturbation stability and on the evolution. This problem is still poorly understood theoretically. It also has a number of important implications for the stability and confinement of ignition and reactor plasmas.

The plasma rotation problem is complex and not well understood. It is well known that toroidal effects tend to damp plasma poloidal rotation, e.g.,

⁶⁶ W. Park, S. Parker, H. Bigliari, and L. Sugiyama, *Phys. Fluids B* 4: 2033 (1992); W. Park, and L. Sugiyama, Numerical Tokamak Workshop 1995, Incline Village, Nevada, April 5-6, 1995.

⁶⁷ L.E. Sugiyama and W. Park, *Two-Fluid 3D Model for Toroidal Plasmas*, MIT RLE Report PTP-96/2, in preparation; L.E. Sugiyama, "3D Two-Fluid Simulation of Tokamak Plasmas," invited paper, American Physical Society Division of Plasma Physics Meeting, 1996; *Bull. Am. Phys. Soc.* 41: 1584 (1996).

⁶⁸ L.E. Sugiyama and W. Park, International Sherwood Fusion Theory Meeting 1995, Incline Village, Nevada, April 1995, paper 1C13; L.E. Sugiyama, "3D Two-Fluid Simulation of Tokamak Plasmas," invited paper, American Physical Society Division of Plasma Physics Meeting, 1996; *Bull. Am. Phys. Soc.* 41: 1584 (1996).

⁶⁹ L.E. Sugiyama, invited paper, American Physical Society Division of Plasma Physics Meeting, 1996; *Bull. Am. Phys. Soc.* 41: 1584 (1996).

Stix⁷⁰ and Hassam and Kulsrud,⁷¹ but there is disagreement about the rate of damping. Competing effects also exist. In the presence of resistivity, analytic results have predicted⁷² that poloidal rotation is unstable and should speed up to a critical speed $v_c = v_s \varepsilon / q$, where $v_s = (T_e/m_i)^{1/2}$ is the sound speed and $\varepsilon = r/R$. A shock forms at an angle θ_s as the rotational speed approaches the critical speed,⁷³ where θ_s varies from π to $-\pi$, depending on the degree of approach and its sign.⁷⁴ Other forms of dissipation can stabilize the rotation at slightly different values, or in other regimes.

All earlier toroidal studies have used simplified descriptions of the plasma configuration, either aspect ratio expansion or reduced equations. The effect is to introduce a local approximation into the analysis. In addition, the orderings have been chosen that neglect radial gradients and the radial propagation of waves. The previous MHD numerical studies have either used equivalent simplifications of the geometry⁷⁵ or, if fully toroidal, have assumed a fixed density profile. In fact, almost no work on rotation has been done with the existing fully toroidal MHD codes.

We have found that the plasma rotation in a finite aspect ratio torus behaves very differently from the existing theoretical predictions. A number of different phenomena occur. These new effects have significant consequences for plasma rotation and also for plasma stability and confinement. As a preliminary step, we have also verified that in the cylinder, the rotation behavior seem to follow the existing theoretical analysis.

1.3.7 Nonlinear Saturation of the Parallel Velocity Shear Instability

Examples abound in laboratory and space plasmas where there are inhomogeneous flows in the direction of the magnetic field—axial flows in linear devices (e.g., Q-machines), plasma rotation due to momentum deposition from neutral beams in tokamaks, deflection and flow of the solar wind along the flanks of a planet's magnetosphere, "precipitation" of plasma onto the ionospheric polar cap along auroral magnetic field lines, etc. Often, these flows exhibit a variation in the direction perpendicular to the B-field, $\bar{\mathbf{B}} \times \nabla V \neq 0$, and this nonuniformity provides excitation energy for instabilities to develop.⁷⁶ A new class of modes⁷⁷ that have a low and realistic excitation threshold have been deemed to play an important role in the transport of momentum and energy in toroidal magnetically confined plasmas. In particular the issue of momentum transport occurring at a rate that is larger than that predicted by the collisional theory has been analyzed and correlated with the ion energy transport in a series of experiments carried out by the TFTR machine.⁷⁸

Linear stability analysis predicts two very distinct limits for the velocity shear problem. With relatively large values of the velocity gradient, a mode first found by D'Angelo⁷⁶ can occur. This mode is characterized by $\gamma \gg \omega_r$, but is easily stabilized in the presence of significant density gradients. A new dissipative instability can occur for relatively low values of the velocity gradient as first suggested by Coppi.⁷⁹ The relevant dissipation can enter through a parallel ion viscosity or ion-neutral collisions. This mode is characterized by $\omega_r \sim \omega_s \gg \gamma$ and is not stabilized by the presence of density gradients. In

⁷⁰ T.H. Stix, *Phys. Rev. Lett.* 16: 1260 (1973).

⁷¹ A.B. Hassam and R. Kulsrud, *Phys. Fluids* 21: 2271 (1978).

⁷² T.E. Stringer, *Phys. Fluids* 13: 810 (1970); R.D. Hazeltine, E.P. Lee, and M.N. Rosenbluth, *Phys. Rev. Lett.* 25: 427 (1970); *Phys. Fluids* 14: 361 (1971).

⁷³ R.D. Hazeltine, E.P. Lee, and M.N. Rosenbluth, *Phys. Rev. Lett.* 25: 427 (1970); *Phys. Fluids* 14: 361 (1971).

⁷⁴ K.C. Shaing, R.D. Hazeltine, and H. Sanuki, *Phys. Fluids* 4: 404 (1985).

⁷⁵ N.K. Winsor, J.L. Johnson, J.M. Dawson, *J. Comp. Phys.* 6: 430 (1970); J.M. Greene, J.L. Johnson, K.E. Wiemer, N.K. Winsor, *Phys. Fluids* 14: 1258 (1971).

⁷⁶ N. D'Angelo, *Phys. Fluids* 8: 1748 (1965).

⁷⁷ B. Coppi, MIT-RLE Report PTP-90/2 (Cambridge, MIT, 1989); B. Coppi, *Plasma Phys. Contr. Fusion* 36: B107 (1994).

⁷⁸ S.D. Scott, V. Arunasalam, and C.W. Barnes et al., *Phys. Fluids* 2: 1300 (1990).

⁷⁹ B. Coppi, MIT-RLE Report PTP-90/2 (Cambridge, MIT, 1989).

driven systems, saturation by quasilinear processes such as relaxation of the velocity gradient is not appropriate, thus one is led to consider other processes such as the coupling to a damped mode.⁸⁰

Thus we have analyzed a model involving a coupling of this kind and found that for this weakly growing dissipative mode, saturation occurs at weak to moderate levels of the mode amplitude.⁸¹

⁸⁰ T.D. Rognlien and J. Weinstock, *J. Geophys. Res.* 79: 4733 (1974); A.B. Hassam, W. Hall, J.D. Huba, and M.J. Keskinen, *J. Geophys. Res.* 91: 13513 (1986).

⁸¹ S. Migliuolo, W. Daughton, B. Coppi, "Nonlinear Saturation of the Parallel Velocity Shear Instability," in *Proceedings of the International Sherwood Theory Conference*, Philadelphia, Pennsylvania, March 18-20, 1996, paper 1D11.